

Constrained Distributed Optimization: A Population Dynamics Approach [★]

Julian Barreiro-Gomez ^{a,b}, Nicanor Quijano ^a, Carlos Ocampo-Martinez ^b

^a*Departamento de Ingeniería Eléctrica y Electrónica, Universidad de los Andes, Carrera 1 No 18A-10, Bogotá Colombia*

^b*Automatic Control Department, Universitat Politècnica de Catalunya, Institut de Robòtica i Informàtica Industrial (CSIC-UPC), Llorens i Artigas, 4-6, 08028 Barcelona, Spain*

Abstract

Large-scale network systems involve a large number of states, which makes the design of real-time controllers a challenging task. A distributed controller design allows to reduce computational requirements since tasks are divided into different systems, allowing real-time processing. This paper proposes a novel methodology for solving constrained optimization problems in a distributed way inspired by population dynamics. This methodology consists of an extension of a population dynamics equation and the introduction of a mass dynamics equation. The proposed methodology divides the problem into smaller sub-problems, whose feasible regions vary over time achieving an agreement to solve the global problem. The methodology also guarantees attraction to the feasible region and allows to have few changes in the decision-making design when a network suffers the addition/removal of nodes/edges. Then, distributed controllers are designed with the proposed methodology and applied to the large-scale Barcelona Drinking Water Network (BDWN). Some simulations are presented and discussed in order to illustrate the control performance.

Key words: Distributed optimization, evolutionary game theory, large-scale systems

1 Introduction

An approach to design control systems is to express the desired performance of the plant as an optimization problem with multiple constraints, e.g., minimization of the error, minimization of the norm of states, minimization of the energy associated to control actions, all of those objectives subject to physical and/or operational constraints. When the system involves a large number of states, the design of optimization-based controllers becomes challenging, because of the lack of centralized information or because of other implications associated to information (e.g., communication issues, costs, reliability). The limitation regarding information availability demands the development of distributed optimization techniques that achieve an optimal point of a performance cost function for the total system by using only local and partial information. There are many distributed optimization applications in engineering, and most of them using a network systems approach [4,5,24,25]. These problems have been solved by using distributed optimization algorithms based on the Newton method [9,27], the sub-gradient method [10,30], and the consensus protocol [10,16,29], among other techniques.

On the other hand, game theory studies the interaction of decision makers and the interconnection of decision making elements based on local information. From this perspective, game-theoretical tools become very useful to describe the behavior of distributed engineered systems [15]. One important characteristic of this theoretical approach is the

[★] This work has been partially supported by the projects “Drenaje urbano y cambio climático: hacia los sistemas de alcantarillado del futuro. Colciencias 548/2012”, and ECOCIS (Ref. DPI2013-48243-C2-1-R). Julian Barreiro-Gomez is supported by COLCIENCIAS-COLFUTURO and by the Agència de Gestió d’Ajust Universitaris i de Recerca AGAUR.

Email addresses: j.barreiro135@uniandes.edu.co - jbarreiro@iri.upc.edu (Julian Barreiro-Gomez), nquijano@uniandes.edu.co (Nicanor Quijano), cocampo@iri.upc.edu (Carlos Ocampo-Martinez).

Nash equilibrium concept, which describes how a global objective is reached based only on local decisions. The task to reach a global objective with partial information is one of the main aspects in distributed optimization problems. This problem may be seen as a multi-agent case in which there are local interactions among them. Furthermore, evolutionary game theory describes the previously mentioned model of agents interacting but also considering a determined population structure, i.e., constraints in the interaction among agents [17]. From this point of view, this theory is suitable to design intelligent systems and controllers for systems where there are local decision makers (local controllers) and achieving a global performance and/or global goal under a specific structure, which is given by the topology of the system (e.g., energy networks, water networks, transportation networks, etc). Also, game theory has become an important and powerful tool for solving optimization problems since the Nash equilibrium corresponds to the extreme of a potential function satisfying the Karush-Kuhn-Tucker (KKT) first order condition [23]. This property is commonly used in a class of games known as potential games, which have gotten special importance in the solution of engineering problems. For instance, in [14] potential games are widely studied from the perspective of state-based games. Furthermore, some kind of optimization problems can be solved by finding a Nash equilibrium for an appropriate designed game, and the consideration of only local information allows to solve distributed optimization problems [1]. For instance, in [6] a distributed convergence to Nash equilibria in two networks is discussed for zero-sum games. In [22], distributed optimization has been applied using replicator dynamics (one of the six fundamental population dynamics), based on local information. In [13], the design of utility functions for each agent in order to decouple constraints is presented, and the usage of penalty functions and barrier functions is discussed. The design of local control laws for individual agents to achieve a global objective is proposed in [12], which has been extended in [28] by using matrix theory.

The consideration of dynamics in the system-equivalent graph that describes information sharing among decision variables is paramount since some network systems in engineering might grow (e.g., drainage network systems, drinking water networks, distributed generation systems). These dynamics represent an addition or removal of elements to/from the network. Moreover, the connectivity of the network elements could change over time (e.g., re-configuration systems), which could affect availability of information. In [11], variations on the graph that determines the system information sharing are studied, where the set of communication links varies with a certain probability.

The main contribution of this paper is to introduce a novel methodology to solve constrained optimization problems in a distributed way, inspired by the population dynamics studied in [23]. Different from the already published population dynamics approaches, this method adds dynamics to the population masses, making the population simplex vary properly over time making the method robust [2]. The method consists in considering the global problem as a society, where there is limitation of information sharing. The society is divided into several populations, where there is full available information. Then, a local optimization problem is solved at each population whose feasible region varies dynamically, i.e., there is an interchange of masses among populations. The feasible regions vary until all populations agree to solve the global optimization problem. In addition to this, applications in the control field may involve disturbances that could lead the trajectories to leave the feasible region (given by constraints that impose a desire performance) [3]. Another relevant difference with respect to already published distributed population dynamics approaches is that the proposed method guarantees that the feasible region is attractive. The last mentioned feature potentially improve the control performance rejecting disturbances. Finally, the design of the decision-making distributed system allows to have a reduced number of modifications when the graph topology changes, i.e., there are new nodes/edges in the graph or there are nodes/edges that disappear. Also, some redundant links can be identified, i.e., links in the graph that are not necessary in the connection among cliques.

The remainder of the paper is organized as follows. Section 2 shows preliminaries of graphs, population dynamics, and introduces the mathematical formalism that is used throughout the paper. Section 3 presents the population dynamics and the mass dynamics, including relevant characteristics. Then, the stability of the dynamics are presented in Section 4. Section 5 shows the different possible changes that the social graph might suffer, and explains the implication over the design. Section 6 presents the optimization problem forms that could be solved with the population dynamics and the mass dynamics, presenting also some illustrative examples and results. Afterwards, the robustness of the method is shown by applying disturbances in Section 7. Then, Section 8 presents a large-scale system and the design of optimal controllers by using the proposed methodology. Controllers consider both a model-based approach, and a model-free approach. Section 9 shows the results and discussion about the performance of controllers designed with the proposed methodology. In Section 10 the main conclusions are drawn.

Notation

The sub-index is associated to a node of a graph, or to a strategy in a game. On the other hand, the super-index refers to a population. For instance, the sub-index i in x_i , \mathcal{P}_i , x_i^p or F_i refers either to a node in a graph or to a strategy,

and the super-index p in m^p , \mathbf{x}^p , x_i^p or N^p indicates a population. Also it should be clear that the super-index is not an operational number, i.e., N^3 refers to population three but $N^3 \neq NNN$. We use bold font for column vectors and matrices, e.g., \mathbf{x} , and \mathbf{H} ; and non-bold style is used for scalar numbers, e.g., N^p . Calligraphy style is used for sets, e.g., \mathcal{S} . The column vector with N unitary entries is denoted by $\mathbf{1}_N$, and the column vector with null entries and suitable dimension is denoted by $\mathbf{0}$. The identity matrix with dimension $N \times N$ is denoted by \mathbb{I}_N . The cardinality of a set \mathcal{S} is denoted by $|\mathcal{S}|$. The continuous time is denoted by t , and it is mostly omitted throughout the manuscript in order to simplify the notation. Finally, \mathbb{R}_+ represents the set of all non-negative real numbers, and \mathbb{Z}_+ represents the set of positive integer numbers.

2 Preliminaries

Let $\mathcal{G} = (\mathcal{V}, \mathcal{E})$ be an undirected non-complete connected graph that exhibits the topology of a society, where \mathcal{V} is the set of vertices of \mathcal{G} that represents the set of N available strategies in a social game denoted by $\mathcal{S} = \{1, \dots, N\}$; and $\mathcal{E} \subset \{(i, j) : i, j \in \mathcal{V}\}$ is the set of edges of \mathcal{G} that determines the possible interactions among society strategies. The graph \mathcal{G} is divided into M sub-complete graphs known as cliques (a complete sub-graph), where each clique represents a population within the society. The set of populations is denoted by $\mathcal{P} = \{1, \dots, M\}$, and the set of cliques is denoted by $\mathcal{C} = \{\mathcal{C}^p : p \in \mathcal{P}\}$. The clique of the population $p \in \mathcal{P}$ is a graph given by $\mathcal{C}^p = (\mathcal{V}^p, \mathcal{E}^p)$, where the set \mathcal{V}^p represents the set of N^p available strategies in a population game denoted by $\mathcal{S}^p = \{i : i \in \mathcal{V}^p\}$, and $\mathcal{E}^p = \{(i, j) : i, j \in \mathcal{V}^p\}$ is the set of all the possible links in \mathcal{C}^p determining full interaction among the population strategies.

It is assumed that cliques are already known, i.e., the number of cliques M , the set of vertices \mathcal{V}^p , and the set of edges \mathcal{E}^p for all $p \in \mathcal{P}$ are known. Although, if it is desired to obtain the optimal set of cliques (i.e., the minimum amount of cliques M such that $\bigcup_{p \in \mathcal{P}} \mathcal{V}^p = \mathcal{V}$, and the minimum amount of links $|\tilde{\mathcal{E}}|$, where $\tilde{\mathcal{E}} = \bigcup_{p \in \mathcal{P}} \mathcal{E}^p \subseteq \mathcal{E}$ such that the graph $\tilde{\mathcal{G}} = (\mathcal{V}, \tilde{\mathcal{E}})$ is connected), there are several methods to find them and it is out of the scope of this paper (e.g., the Bron Kerbosh algorithm). Once the optimal set of cliques \mathcal{C} has been identified, it is possible to find *redundant edges or links*. A link $(i, j) \in \mathcal{E}$ is redundant if $(i, j) \notin \tilde{\mathcal{E}}$, i.e., $(i, j) \notin \mathcal{E}^p$, for all $p \in \mathcal{P}$.

Then, we define the number of cliques that contain a node $i \in \mathcal{V}$ denoted by $G(i)$ as

$$G(i) = \sum_{p \in \mathcal{P}} g(i, p), \quad \text{and} \quad g(i, p) = \begin{cases} 1 & \text{if } i \in \mathcal{V}^p \\ 0 & \text{otherwise.} \end{cases}$$

Since \mathcal{G} is a non-complete connected graph, then all cliques must share at least one node with another clique, which is known as an intersection node. The set of intersection nodes in a population $p \in \mathcal{P}$ is denoted by $\mathcal{I}^p = \{i \in \mathcal{V}^p : G(i) > 1\}$, and the set of intersection nodes in the graph \mathcal{G} is denoted by $\mathcal{I} = \bigcup_{p \in \mathcal{P}} \mathcal{I}^p$.

Proposition 1 *In an optimal set of cliques, two cliques do not share more than one intersection node.*

PROOF. Suppose a society with a topology given by the graph $\mathcal{G} = (\mathcal{V}, \mathcal{E})$, which is composed of M populations, i.e., $\mathcal{P} = \{1, \dots, M\}$. Now, suppose that two cliques associated to populations $p, q \in \mathcal{P}$ share more than one intersection node, i.e., $|\tilde{\mathcal{I}}| > 1$, where $\tilde{\mathcal{I}} = \mathcal{I}^p \cap \mathcal{I}^q$. Then \mathcal{C} is not an optimal set of cliques (i.e., there are redundant links in $\tilde{\mathcal{E}} = \bigcup_{p \in \mathcal{P}} \mathcal{E}^p$). Moreover, \mathcal{C}^p and \mathcal{C}^q are complete graphs with set of vertices \mathcal{V}^p and \mathcal{V}^q , respectively. Suppose without loss of generality that $|\mathcal{V}^p| > |\mathcal{V}^q|$, and that $a, b \in \tilde{\mathcal{I}}$. Finally, notice that all the edges $\{(a, j) \in \mathcal{E} : j \in \mathcal{V}^p \setminus \{\tilde{\mathcal{I}}\}\}$ are redundant edges or links in \mathcal{G} . Consequently, the set of cliques \mathcal{C} is not optimal since the clique \mathcal{C}^p may be reduced to the complete graph $\tilde{\mathcal{C}}^p$, by $\tilde{\mathcal{V}}^p = \mathcal{V}^p \setminus \{a\}$, and $\tilde{\mathcal{E}}^p = \mathcal{E}^p \setminus \{(a, j) : j \in \mathcal{V}^p \setminus \{a\}\}$. ■

Example 2.1 Suppose the social topology composed of three populations $\mathcal{P} = \{1, 2, 3\}$ as shown in Figure 1, where $\mathcal{V}^1 = \{1, 2, 3\}$, $\mathcal{V}^2 = \{1, 3, 4, 5, 6\}$, and $\mathcal{V}^3 = \{6, 7\}$. The sets of intersection nodes for each population are given by $\mathcal{I}^1 = \{1, 3\}$, $\mathcal{I}^2 = \{1, 3, 6\}$, and $\mathcal{I}^3 = \{6\}$. Then, two populations share more than an intersection node, i.e., $\tilde{\mathcal{I}} = \mathcal{I}^1 \cap \mathcal{I}^2 = \{1, 3\} = \{a, b\}$, where $|\tilde{\mathcal{I}}| > |\mathcal{I}^1|$. Then, the redundant links are given by $\{(1, j) : j \in \{1, 3, 4, 5, 6\} \setminus \{1, 3\}\}$, i.e., $\{(1, 4), (1, 5), (1, 6)\}$ as shown in Figure 1 a). Finally, it is obtained the three cliques shown in Figure 1 b) after removing the mentioned redundant links. □

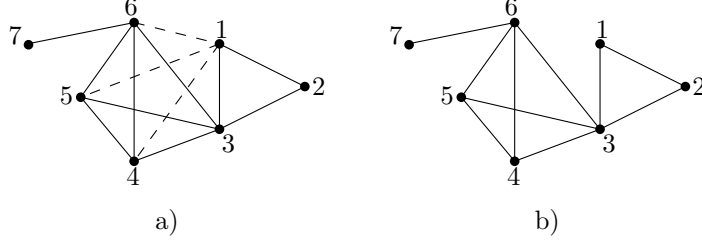


Fig. 1. Population dynamics with more than one intersection node, i.e., non-optimal set of cliques with redundant links.

Throughout the paper, we are going to refer to all the populations $p \in \mathcal{P}$ such that a node $i \in \mathcal{V}$ belongs to the set of nodes \mathcal{V}^p . This is the set of all the populations that includes a certain node $i \in \mathcal{V}$ and it is denoted by $\mathcal{P}_i = \{p : i \in \mathcal{V}^p\}$, where $\mathcal{P}_i \subseteq \mathcal{P}$. For instance, let us consider a simple social topology shown in Figure 1b) with three populations $\mathcal{P} = \{1, 2, 3\}$ whose sets of nodes are given by $\mathcal{V}^1 = \{1, 2, 3\}$, $\mathcal{V}^2 = \{3, 4, 5, 6\}$, and $\mathcal{V}^3 = \{6, 7\}$, respectively. Then, $\mathcal{P}_2 = \{p : 2 \in \mathcal{V}^p\} = \{1\}$, whereas $\mathcal{P}_3 = \{p : 3 \in \mathcal{V}^p\} = \{1, 2\}$, and $\mathcal{P}_6 = \{p : 6 \in \mathcal{V}^p\} = \{2, 3\}$ (node $6 \in \mathcal{V}$ belongs to population 2, and population 3 $\in \mathcal{P}$).

The scalar $x_i \in \mathbb{R}_+$ corresponds to the proportion of agents in the society selecting the strategy $i \in \mathcal{S}$, and the scalar $x_i^p \in \mathbb{R}_+$ is the proportion of agents selecting the strategy $i \in \mathcal{S}^p$ in the population $p \in \mathcal{P}$. Moreover, the distribution of agents throughout the available strategies in the society and populations is known as the social state and the population state denoted by $\mathbf{x} \in \mathbb{R}_+^N$, and $\mathbf{x}^p \in \mathbb{R}_+^{N^p}$, respectively. The set of possible social states is given by a simplex denoted by Δ , which is a constant set, i.e., $\Delta = \{\mathbf{x} \in \mathbb{R}_+^N : \sum_{i \in \mathcal{S}} x_i = m\}$, where $m \in \mathbb{R}_+$ is the constant mass of agents in the society. Similarly, the set of possible states of the population $p \in \mathcal{P}$ is given by a non-constant simplex defined as $\Delta^p = \{\mathbf{x}^p \in \mathbb{R}_+^{N^p} : \sum_{i \in \mathcal{S}^p} x_i = m^p\}$, where $m^p \in \mathbb{R}_+$ corresponds to the mass of agents in the population $p \in \mathcal{P}$. Furthermore, there is a relationship between the social states and the population states given by

$$x_i = \frac{1}{G(i)} \sum_{p \in \mathcal{P}_i} x_i^p. \quad (1)$$

Notice that if it is considered that $x_i^p = 0$ for all $i \notin \mathcal{V}^p$, then (1) can be written as

$$x_i = \frac{1}{G(i)} \sum_{p \in \mathcal{P}} x_i^p. \quad (2)$$

The fitness functions take a social or population state, and return the payoff that a proportion of agents playing a certain strategy receives. Let $F_i : \Delta \mapsto \mathbb{R}$ be the mapping of the fitness function for the proportion of agents playing the strategy $i \in \mathcal{S}$, and $F_i^p : \Delta^p \mapsto \mathbb{R}$ be the mapping of the fitness function for the proportion of agents playing the strategy $i \in \mathcal{S}^p$ in the population $p \in \mathcal{P}$. The fitness corresponding to a strategy $i \in \mathcal{S}$ is the same as the fitness for a strategy $j \in \mathcal{S}^p$ for all $p \in \mathcal{P}$ if $i = j$. Consequently, for all $i \in \mathcal{S}^p$ and for all $p \in \mathcal{P}_i$,

$$F_i(\mathbf{x}) = F_i^p(\mathbf{x}^p), \text{ if } x_i = x_i^p. \quad (3)$$

The vector of the fitness functions for a society is given by $\mathbf{F} = [F_1 \ \dots \ F_N]^\top \in \mathbb{R}^N$. The social average fitness is denoted by \bar{F} , where $\bar{F} = (\mathbf{x}^\top \mathbf{F})/m$. Similarly, the vector of fitness functions for a population $p \in \mathcal{P}$ is given by $\mathbf{F}^p \in \mathbb{R}^{N^p}$, whose fitness functions are associated to the strategies \mathcal{S}^p . The average fitness for a population $p \in \mathcal{P}$ is denoted by $\bar{F}^p = (\mathbf{x}^{p^\top} \mathbf{F}^p)/m^p$. There is a relationship between the population masses and the social mass given by

$$m = \sum_{p \in \mathcal{P}} m^p - \sum_{i \in \mathcal{S}} (G(i) - 1)x_i. \quad (4)$$

Remark 1 *The relationship between the population masses and the social mass presented in (4) guarantees that the simplex Δ is satisfied, i.e., $\sum_{i \in \mathcal{S}} x_i = m$. This required relationship is guaranteed with the mass dynamics presented in the next section, and the implication of the simplex satisfaction obtained with this relationship is analyzed below in the section of stability analysis.* \diamond

The framework of this paper is given by the assumptions stated next.

Assumption 1 The game \mathbf{F} is a full potential game [23], i.e., there is a continuously differentiable function $f(\mathbf{x})$, known as the potential function, satisfying

$$\frac{\partial f(\mathbf{x})}{\partial x_i} = F_i(\mathbf{x}), \text{ for all } i \in \mathcal{S}, \text{ and } \mathbf{x} \in \Delta.$$

Assumption 2 Fitness functions depend only on strategies on which there is connection, i.e., each node requires only available information given by the graph topology.

Assumption 3 The proportion of agents playing the strategies corresponding to intersection nodes are strictly positive for all the time, i.e., $x_i^p > 0$ for all $i \in \mathcal{I}$, and for all $p \in \mathcal{P}$ (i.e., there is not extinction of the intersection population). This also implies that population masses are strictly positive, i.e., $m^p > 0$, for all $p \in \mathcal{P}$, since the population masses are composed of proportion of agents within populations.

Assumption 4 The game \mathbf{F} is a stable game [8], i.e., the Jacobian matrix $D\mathbf{F}(\mathbf{x})$ is negative semi-definite with respect to the tangent space defined as $T\Delta = \{\mathbf{z} \in \mathbb{R}^N : \sum_{i \in \mathcal{S}} z_i = 0\}$, i.e.,

$$\mathbf{z}^\top D\mathbf{F}(\mathbf{x})\mathbf{z} \leq 0, \text{ for all } \mathbf{z} \in T\Delta, \text{ and } \mathbf{x} \in \Delta. \quad (5)$$

The features of the potential function $f(\mathbf{x})$ determine whether the full potential game \mathbf{F} is stable, as shown in Lemma 1.

Lemma 1 If $f(\mathbf{x})$ is twice continuously differentiable and concave, then the full potential game \mathbf{F} is a stable game.

PROOF. Since $f(\mathbf{x})$ is concave, the Hessian matrix $\mathbf{J} = D\mathbf{F}(\mathbf{x})$ is negative semi-definite. Therefore, $\mathbf{z}^\top D\mathbf{F}(\mathbf{x})\mathbf{z} \leq 0$ is satisfied. This condition is the same as in (5). \blacksquare

3 Population and mass dynamics

The objective for the society is to converge to a Nash equilibrium¹ of the game \mathbf{F} denoted by $\mathbf{x}^* \in \Delta$. In order to achieve this objective, there is a game at each population $p \in \mathcal{P}$ converging to a Nash equilibrium of the game \mathbf{F}^p denoted by $\mathbf{x}^{p*} \in \Delta^p$, and the intersection nodes $i \in \mathcal{I}$ allow a mass interchange among the different populations.

3.1 Population dynamics

A game is solved for each population with constraints given by the population masses m^p , which vary dynamically. Dynamics associated to each population are shown in (6a). There are M different dynamics of this form, one for each clique \mathcal{C}^p for all $p \in \mathcal{P}$, i.e.,

$$\dot{x}_i^p = x_i^p (F_i^p - \bar{F}^p - \phi^p), \text{ for all } i \in \mathcal{S}^p, \quad (6a)$$

$$\phi^p = \beta \left(\frac{1}{m^p} \sum_{j \in \mathcal{S}^p} x_j^p - 1 \right), \quad (6b)$$

where β is the convergence factor for the whole system that takes a positive and finite value. Notice that, when $\phi^p = 0$ (i.e., $\mathbf{x}^p \in \Delta^p$), then (6a) becomes the classical replicator dynamics equation. The use of the convergence factor is further discussed in Section 7.

¹ $\mathbf{x}^* \in \Delta$ is a Nash equilibrium if each used strategy entails the maximum benefit for the proportion of agents selecting it, i.e., the set of Nash equilibria is given by $\{\mathbf{x}^* \in \Delta : x_i^* > 0 \Rightarrow F_i(\mathbf{x}^*) \geq F_j(\mathbf{x}^*)\}$, for all $i, j \in \mathcal{S}$ [23].

3.2 Mass dynamics

On the other hand, there are as many mass dynamics as intersection nodes in the graph, i.e., one for each $i \in \mathcal{I}$. The dynamics for population masses m^p are given by

$$\dot{m}_i^p = m_i^p (x_i - x_i^p - \psi_i), \quad \text{for all } p \in \mathcal{P}_i, \quad (7a)$$

$$\psi_i = \beta \left(\frac{1}{\kappa_i + (G(i) - 1) x_i} \sum_{q \in \mathcal{P}_i} \frac{m_i^q}{|\mathcal{I}^q|} - 1 \right), \quad (7b)$$

where $\kappa_i \in \mathbb{R}_+$ is a distribution of the social mass m . Then, it should be satisfied that

$$\sum_{i \in \mathcal{I}} \kappa_i = m. \quad (8)$$

Equation (7a) describes the movements of agents among populations through intersection nodes, and the term β in (7b) is the convergence factor of the system. There might be alternative possibilities in the selection of the mass dynamics (7). However, the requirements that should be satisfied are: i) the dynamics satisfy the communication constraints established by the graph \mathcal{G} , and ii) dynamics converge to the equilibrium point given by the following equality:

$$\kappa_i + (G(i) - 1) x_i^* = \sum_{q \in \mathcal{P}} \frac{m_i^{q*}}{|\mathcal{I}^q|}. \quad (9)$$

Notice that $\sum_{q \in \mathcal{P}_i} \{m_i^q / |\mathcal{I}^q|\} = \sum_{q \in \mathcal{P}} \{m_i^q / |\mathcal{I}^q|\}$ since $m_i^q = 0$, for all $i \notin \mathcal{V}^q$.

In the general case, the selection of the κ_i for all $i \in \mathcal{I}$ is not a trivial problem. This selection is discussed in detail in Section 6, and the selection of κ_i is shown for an example in which the intersection nodes do not form a complete graph within the social topology.

There is a relationship between m_i^p , for all $i \in \mathcal{I}^p$, and the population masses m^p given by

$$m^p = \frac{1}{|\mathcal{I}^p|} \sum_{i \in \mathcal{I}^p} m_i^p, \quad \text{for all } p \in \mathcal{P}. \quad (10)$$

For the mass dynamics at intersection nodes in (7a), the vector of masses and the vector of states associated to an intersection node $i \in \mathcal{I}$ are defined next. The masses vector is denoted by $\mathbf{m}_i = [m_i^{p_1} \ \dots \ m_i^{p_{G(i)}}]^\top \in \mathbb{R}^{G(i)}$, where $p_1, \dots, p_{G(i)} \in \mathcal{P}_i$; and the vector of population states is $\mathbf{x}_i = [x_i^{p_1} \ \dots \ x_i^{p_{G(i)}}]^\top \in \mathbb{R}^{G(i)}$, where $p_1, \dots, p_{G(i)} \in \mathcal{P}_i$; both vectors \mathbf{m}_i , and \mathbf{x}_i for all $i \in \mathcal{I}$. Notice that, $\mathbf{m}_i \neq m_i$, and $\mathbf{x}_i \neq x_i$.

In order to illustrate the structure of the methodology and the interaction between the population dynamics and the mass dynamics, consider the social topology given by the graph $\mathcal{G} = (\mathcal{V}, \mathcal{E})$, where $\mathcal{V} = \{1, 2, 3, 4, 5\}$, and $\mathcal{E} = \{\{1, 2\}, \{1, 3\}, \{2, 3\}, \{3, 4\}, \{3, 5\}, \{4, 5\}\}$. For this society, there are two populations and only one intersection node. consequently, $\mathcal{I}^1 = \mathcal{I}^2 = \mathcal{I} = \{3\}$. The structure for this problem is shown in Figure 2.

3.3 Population game without social mass constraint

Now, suppose the case in which it is desired to achieve a Nash equilibrium, but without imposing a social mass, i.e., there is not limitation in the growth of agents within the society. Notice that, since it is not necessary to satisfy a determined social mass, then (9) is not longer required. Consequently, the term ψ_i in (7a) is not necessary. Then, the mass dynamics are changed and rewritten as follows:

$$\dot{m}_i^p = m_i^p (x_i - x_i^p), \quad \text{for all } p \in \mathcal{P}_i. \quad (11)$$

Besides, even though ψ_i is not present, the equilibrium \mathbf{m}_i^* still implies that $x_i = x_i^p$ for all $p \in \mathcal{P}_i$ and $i \in \mathcal{I}$. Also, the whole system still converges to a Nash equilibrium since the population dynamics are the same. However, the social mass m and the average fitness F take arbitrary values at equilibrium.

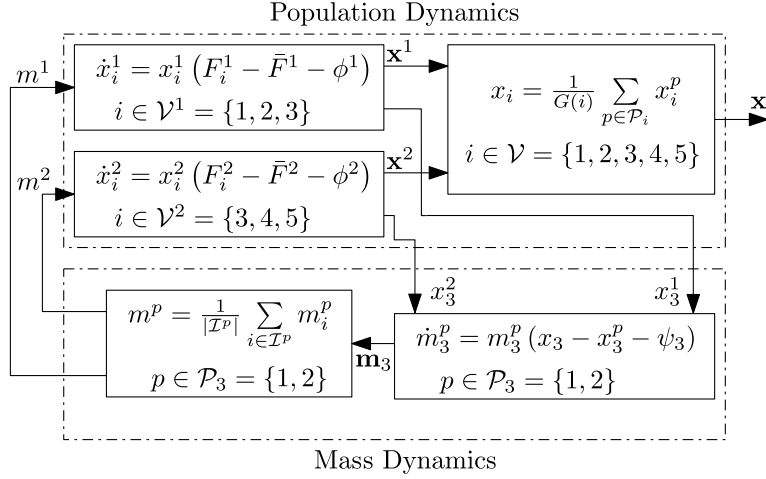


Fig. 2. The methodology structure with two populations and one mass dynamics.

The dynamical system can be forced to converge to a Nash equilibrium \mathbf{x}^* such that $\mathbf{F}(\mathbf{x}^*) = \nabla f(\mathbf{x}^*)$ converges to a desired value $F_i(r)$ for an $i \in \mathcal{I}$, where r is a known value (e.g., a reference). Modifying the relationship between the states in (2) by adding the reference r , the following new relationship is obtained:

$$x_i = \frac{1}{G(i) + 1} \left(\sum_{p \in \mathcal{P}} x_i^p + r \right),$$

where $x_i^p = 0$, if $i \notin \mathcal{V}^p$. Using this modification, by (11), x_i tends to r . This makes \bar{F} to converge to the desired value $F_i(r)$, for only one $i \in \mathcal{I}$.

Remark 2 In case that r is not easily found for any $i \in \mathcal{I}$, it is possible to establish a known decreasing auxiliary function denoted by $\tilde{F}_{N+1}(x_{N+1})$, where x_{N+1} is an auxiliary intersection node that is not part of the optimization problem. Reference r is known, so that $\tilde{F}(r)$ is the desired value for the average fitness. The addition of a new variable does not affect the solution, but forces trajectories towards a desired value. \diamond

4 Stability analysis

It is necessary to show that the solution of the distributed system with population dynamics (6a), and mass dynamics (7a) at intersection nodes, implies the solution of the social game (i.e., the global problem).

Proposition 2 If Assumption 3 is satisfied, the population dynamics (6a) are in equilibrium ($\mathbf{x}^{p*} \in \Delta^p$, for all $p \in \mathcal{P}$), and the mass dynamics (7a) are in equilibrium (\mathbf{m}_i^* , for all $i \in \mathcal{I}$); then, the society is in equilibrium, i.e., $\mathbf{x}^* \in \Delta$.

PROOF. The equilibrium $\mathbf{x}^{p*} \in \Delta^p$ of the population dynamics (6a), for all $p \in \mathcal{P}$, implies that

- i) $\phi^p(\mathbf{x}^{p*}) = 0$, and,
- ii) $F_i^p(\mathbf{x}^{p*}) = \bar{F}^p$, for all $i \in \mathcal{S}^p$, and $p \in \mathcal{P}$.

The equilibrium \mathbf{m}_i^* of the mass dynamics (7a), for all $i \in \mathcal{I}$, implies that

- i) $\psi_i(x_i^*, \mathbf{m}_i^*) = 0$ since (9) is forced, and,
- ii) $x_i^* = x_i^{p*}$ for all $p \in \mathcal{P}_i$.

Then, for all $i \in \mathcal{I}$, $x_i^* = x_i^{s*} = x_i^{k*}$, for all $s, k \in \mathcal{P}_i$. By (3) $F_i(\mathbf{x}^{s*}) = F_i(\mathbf{x}^{k*}) = F_i(\mathbf{x}^*)$. Moreover, $F_i(\mathbf{x}^{s*}) = \bar{F}^s(\mathbf{x}^{r*}) = F_i(\mathbf{x}^{k*}) = \bar{F}^k(\mathbf{x}^{k*})$, for all $s, k \in \mathcal{P}$ and $i \in \mathcal{I}$. Consequently, all population average fitnesses are equal,

then $F_i(\mathbf{x}^*) = F_j(\mathbf{x}^*) = \bar{F}(\mathbf{x}^*)$ for all $i, j \in \mathcal{S}$. Additionally, \mathbf{m}_i^* for all $i \in \mathcal{I}$ satisfies (9). Then,

$$\sum_{i \in \mathcal{I}} (\kappa_i + (G(i) - 1)x_i^*) = \sum_{i \in \mathcal{I}} \sum_{p \in \mathcal{P}} \frac{m_i^p}{|\mathcal{I}^p|}.$$

By (10), and using the fact that $m_i^p = 0$, if $i \notin \mathcal{I}^p$

$$\sum_{i \in \mathcal{I}} \kappa_i + \sum_{i \in \mathcal{I}} (G(i) - 1)x_i^* = \sum_{p \in \mathcal{P}} m^p.$$

For a node $i \notin \mathcal{I}$, $G(i) = 1$, and by (8)

$$m + \sum_{i \in \mathcal{S}} (G(i) - 1)x_i^* = \sum_{p \in \mathcal{P}} m^p,$$

since $\mathbf{x}^{p*} \in \Delta^p$, and owing that $x_i^p = 0$, for all $i \notin \mathcal{V}^p$

$$\begin{aligned} m + \sum_{i \in \mathcal{S}} (G(i) - 1)x_i^* &= \sum_{p \in \mathcal{P}} \sum_{i \in \mathcal{S}^p} x_i^{p*}, \\ &= \sum_{p \in \mathcal{P}} \sum_{i \in \mathcal{S}} x_i^{p*}. \end{aligned}$$

Finally, by (2),

$$\begin{aligned} m + \sum_{i \in \mathcal{S}} (G(i) - 1)x_i^* &= \sum_{i \in \mathcal{S}} G(i)x_i^*, \\ m &= \sum_{i \in \mathcal{S}} x_i^*. \end{aligned}$$

Then $\mathbf{x}^* \in \Delta$ completes the proof. ■

Next, it is shown that the equilibrium points corresponding to the population dynamics and the mass dynamics are asymptotically stable. Then, the population and mass dynamics will converge to a solution under the conditions set in Theorem 1.

Theorem 1 *If \mathbf{F} is a stable game, then there exists a β such that the equilibrium point $\mathbf{x}^{p*} \in \Delta^p$ of the population dynamics (6a), for all $p \in \mathcal{P}$, and the equilibrium point \mathbf{m}_i^* of the mass dynamics (7a), for all $i \in \mathcal{I}$, are asymptotically stable.*

PROOF. Consider the Lyapunov function

$$V(\mathbf{x}^p, \mathbf{m}_i) = \sum_{p \in \mathcal{P}} \sum_{i \in \mathcal{S}^p} \left(x_i^p - x_i^{p*} \left(1 + \ln \left(\frac{x_i^p}{x_i^{p*}} \right) \right) \right) + \sum_{i \in \mathcal{I}} \sum_{p \in \mathcal{P}_i} \left(m_i^p - m_i^{p*} \left(1 + \ln \left(\frac{m_i^p}{m_i^{p*}} \right) \right) \right), \quad (12)$$

which is convex for non-negative proportion of agents and masses, i.e., $\mathbf{x}^p \in \mathbb{R}_+^{N^p}$, for all $p \in \mathcal{P}$, and $\mathbf{m}_i \in \mathbb{R}_+^{G(i)}$, for all $i \in \mathcal{I}$. Moreover,

- $V(\mathbf{x}^{p*}, \mathbf{m}_i^*) = 0$,
- $V(\mathbf{x}^p, \mathbf{m}_i) > 0$ if $\mathbf{x}^p \neq \mathbf{x}^{p*}$ or $\mathbf{m}_i \neq \mathbf{m}_i^*$,

and its derivative is given as

$$\dot{V}(\mathbf{x}^p, \mathbf{m}_i) = \underbrace{\sum_{p \in \mathcal{P}} \sum_{i \in \mathcal{S}^p} \left(1 - \frac{x_i^{p*}}{x_i^p}\right) \dot{x}_i^p}_{V_1} + \underbrace{\sum_{i \in \mathcal{I}} \sum_{p \in \mathcal{P}_i} \left(1 - \frac{m_i^{p*}}{m_i^p}\right) \dot{m}_i^p}_{V_2}.$$

Consider the vector $\mathbf{I}_i = \left[\frac{1}{|\mathcal{I}^p|} \quad \dots \quad \frac{1}{|\mathcal{I}^{p_{G(i)}}|} \right]^\top \in \mathbb{R}^{G(i)}$, where $p_1, \dots, p_{G(i)} \in \mathcal{P}_i$, and $i \in \mathcal{I}$; and the change of variable $\tilde{\kappa}_i = \kappa_i + (G(i) - 1)x_i$, where $\tilde{\kappa}_i > 0$. Then,

$$\dot{V}(\mathbf{x}^p, \mathbf{m}_i) = V_1 + V_2,$$

where

$$V_1 = \sum_{p \in \mathcal{P}} \left\{ (\mathbf{x}^p - \mathbf{x}^{p*})^\top \left(\mathbf{F}^p(\mathbf{x}^p) - \frac{1}{m^p} \mathbf{1}_{N^p} \mathbf{x}^{p\top} \mathbf{F}^p(\mathbf{x}^p) - \frac{\beta}{m^p} \mathbf{1}_{N^p} \mathbf{x}^{p\top} \mathbf{1}_{N^p} + \mathbf{1}_{N^p} \beta \right) \right\},$$

$$V_2 = \sum_{i \in \mathcal{I}} \left\{ (\mathbf{m}_i - \mathbf{m}_i^*)^\top \left(\mathbf{1}_{G(i)} \mathbf{x}_i^\top \mathbf{1}_{G(i)} \frac{1}{G(i)} - \mathbf{x}_i - \mathbf{1}_{G(i)} \mathbf{m}_i^\top \mathbf{I}_i \frac{\beta}{\tilde{\kappa}_i} + \mathbf{1}_{G(i)} \beta \right) \right\}.$$

Since it is possible that in a transitory event $\mathbf{x}^p \notin \Delta^p$, then we consider that $\mathbf{x}^{p\top} \mathbf{1}_{N^p} = m^p + \epsilon$. The parameter ϵ could be either positive or negative depending on \mathbf{x}^p . Moreover, it is known that $\mathbf{x}^{p*} \in \Delta^p$, then $\mathbf{x}^{p*\top} \mathbf{1}_{N^p} = m^p$.

In the same way, it is possible that, in a transitory event, \mathbf{m}_i does not satisfy the condition in (9) (i.e., $\mathbf{m}_i^\top \mathbf{I}_i \neq \tilde{\kappa}_i$). Then, $\mathbf{m}_i^\top \mathbf{I}_i = \tilde{\kappa}_i + \gamma$, where γ could be either positive or negative depending on the condition in (9). Finally, since $|\mathcal{I}^p| \geq 1$, for all $p \in \mathcal{P}$,

$$\begin{aligned} \tilde{\kappa}_i + \gamma &= \mathbf{m}_i^\top \mathbf{I}_i \\ &= \sum_{p \in \mathcal{P}} \frac{m_i^p}{|\mathcal{I}^p|} \\ &\leq \sum_{p \in \mathcal{P}} m_i^p \\ &= \mathbf{m}_i^\top \mathbf{1}_{G(i)} \\ &= \tilde{\kappa}_i + \gamma + \theta, \end{aligned}$$

where $\theta \geq 0$. Replacing $\mathbf{x}^{p\top} \mathbf{1}_{N^p}$, $\mathbf{x}^{p*\top} \mathbf{1}_{N^p}$, $\mathbf{m}_i^\top \mathbf{I}_i$, and $\mathbf{m}_i^\top \mathbf{1}_{G(i)}$. Then, $\dot{V}(\mathbf{x}^p, \mathbf{m}_i)$ is written as

$$\dot{V}(\mathbf{x}^p, \mathbf{m}_i) = \sum_{p \in \mathcal{P}} \left\{ \left(1 - \frac{m^p + \epsilon}{m^p}\right) \mathbf{x}^{p\top} \mathbf{F}^p(\mathbf{x}^p) - \beta \frac{\epsilon^2}{m^p} + (\mathbf{x}^p - \mathbf{x}^{p*})^\top \mathbf{F}^p(\mathbf{x}^p) \right\} + \sum_{i \in \mathcal{I}} \left\{ \frac{\gamma}{G(i)} \mathbf{x}_i^\top \mathbf{1}_{G(i)} + (\mathbf{m}_i^* - \mathbf{m}_i)^\top \mathbf{x}_i - \beta \frac{\gamma^2}{\tilde{\kappa}_i} \right\}. \quad (13)$$

There are some cases to analyze:

i) $\epsilon = 0$ and $\gamma = 0$. Then $\dot{V}(\mathbf{x}^p, \mathbf{m}_i) = \sum_{p \in \mathcal{P}} (\mathbf{x}^p - \mathbf{x}^{p*})^\top \mathbf{F}^p(\mathbf{x}^p) + \sum_{i \in \mathcal{I}} (\mathbf{m}_i^* - \mathbf{m}_i)^\top \mathbf{x}_i$. The first term is negative since $\mathbf{F}(\mathbf{x}^p)$ is a stable game. The second term is also negative since all fitness functions have the same decreasing tendency (e.g., Figure 3 shows a geometric notion with two population with an intersection). Therefore, $\dot{V}(\mathbf{x}^p, \mathbf{m}_i) \leq 0$.

ii) In all other cases, there exists a β such that $\dot{V}(\mathbf{x}^p, \mathbf{m}_i) \leq 0$. For the case $\epsilon \neq 0$ and $\gamma \neq 0$, β is given by

$$\beta \geq \frac{1}{\left(\sum_{p \in \mathcal{P}} \frac{\epsilon^2}{m^p} + \sum_{i \in \mathcal{I}} \frac{\gamma^2}{\tilde{\kappa}_i} \right)} \left\{ \sum_{p \in \mathcal{P}} \left\{ \left(1 - \frac{m^p + \epsilon}{m^p}\right) \mathbf{x}^{p\top} \mathbf{F}^p(\mathbf{x}^p) + (\mathbf{x}^p - \mathbf{x}^{p*})^\top \mathbf{F}^p(\mathbf{x}^p) \right\} + \sum_{i \in \mathcal{I}} \left\{ \frac{\gamma}{G(i)} \mathbf{x}_i^\top \mathbf{1}_{G(i)} + (\mathbf{m}_i^* - \mathbf{m}_i)^\top \mathbf{x}_i \right\} \right\}.$$

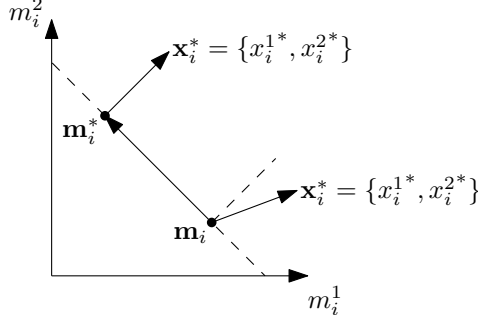


Fig. 3. Geometric notion for the masses and the states in an intersection node, where $G(i) = 2$ with $i \in \mathcal{I}$.

This bound determines the magnitude of the convergence factor such that the trajectories are forced to remain into the feasible region. Notice that, when the population states are near the feasible region (i.e., $\epsilon \rightarrow 0$, and $\gamma \rightarrow 0$), the convergence factor is not longer required (i.e., β can get any positive value).

In (13), the equality $\dot{V}(\mathbf{x}^p, \mathbf{m}_i) = 0$ holds when $\mathbf{x}^p = \mathbf{x}^{p*}$ and $\mathbf{m}_i = \mathbf{m}_i^*$ (Case *i*). Applying LaSalle's invariance principle, every solution starting in $\mathbf{x}^p(0) \in \mathbb{R}_+^{N^p}$ and $\mathbf{m}_i(0) \in \mathbb{R}_+^{G(i)}$ approaches to \mathbf{x}^{p*} and \mathbf{m}_i^* as $t \rightarrow \infty$. ■

Remark 3 Proof of Theorem 1 also shows that the feasible region is attractive, i.e., if disturbances affecting the system make the trajectories to leave the feasible region, then the distributed system composed of population and mass dynamics forces trajectories to converge to a feasible solution. ◇

When there is a population game without a social mass constraint, both the mass dynamics and the relationship between states change. Then, it is necessary to show stability for the new dynamical system.

Theorem 2 If \mathbf{F} is a stable game, then there exists a β such that the equilibrium \mathbf{x}^{p*} of the population dynamics (6a) for all $p \in \mathcal{P}$, and the equilibrium \mathbf{m}_i^* of the mass dynamics (11) for all $i \in \mathcal{I}$ is asymptotically stable.

PROOF. For this proof, the Lyapunov function in (12) is used. Moreover, a change of variable is made given by $\tilde{\mathbf{x}}_i = \mathbf{1}_{G(i)}[\mathbf{x}_i^\top \quad r] \mathbf{1}_{[G(i)+1]} \frac{1}{G(i)+1}$. Then,

$$\dot{V}(\mathbf{x}^p, \mathbf{m}_i) = \sum_{p \in \mathcal{P}} \left\{ \left(1 - \frac{m^p + \epsilon}{m^p} \right) \mathbf{x}^{p\top} \mathbf{F}^p(\mathbf{x}^p) - \beta \frac{\epsilon^2}{m^p} + (\mathbf{x}^p - \mathbf{x}^{p*})^\top \mathbf{F}^p(\mathbf{x}^p) \right\} + \sum_{i \in \mathcal{I}} \{ (\mathbf{m}_i^* - \mathbf{m}_i)^\top (\mathbf{x}_i - \tilde{\mathbf{x}}_i) \},$$

where $\dot{V}(\mathbf{x}^p, \mathbf{m}_i) \leq 0$ when $\epsilon = 0$. There exists a β for $\epsilon \neq 0$, such that $\dot{V}(\mathbf{x}^p, \mathbf{m}_i) \leq 0$, given by

$$\beta \geq \frac{1}{\sum_{p \in \mathcal{P}} \frac{\epsilon^2}{m^p}} \left\{ \sum_{p \in \mathcal{P}} \left\{ \left(1 - \frac{m^p + \epsilon}{m^p} \right) \mathbf{x}^{p\top} \mathbf{F}^p(\mathbf{x}^p) + (\mathbf{x}^p - \mathbf{x}^{p*})^\top \mathbf{F}^p(\mathbf{x}^p) \right\} + \sum_{i \in \mathcal{I}} \{ (\mathbf{m}_i^* - \mathbf{m}_i)^\top (\mathbf{x}_i - \tilde{\mathbf{x}}_i) \} \right\}.$$

This bound determines the magnitude of the convergence factor such that the trajectories are forced to remain into the feasible region. Notice that, when the population states are near the feasible region (i.e., $\epsilon \rightarrow 0$), the convergence factor is not longer required (i.e., β can get any positive value). ■

5 Changes in the graph

Network systems in engineering are constantly growing. On the other hand, some systems isolate a segment of the network under some specific conditions (e.g., an operation fault), and this might suppose a reduction in the graph. When any of these two situations occur, the controller should be re-designed in order to fit the new system conditions. The method proposed in this paper allows to reduce the number of changes in the original design when changes in the graph are made. It is necessary to highlight that the modifications over the graph should not disconnect the

graph, i.e., the removal of an intersection node is not allowed in an optimal set of cliques since this would disconnect the social topology graph according to Proposition 1 (two cliques only share one intersection node). In order to illustrate this property of the methodology, we analyze different cases of addition and/or removal of vertices and/or edges to/from the original graph (i.e., the graph that has been previously used for the control design). We discuss different possible situations, and Figure 4 shows a simple example for each one of them.

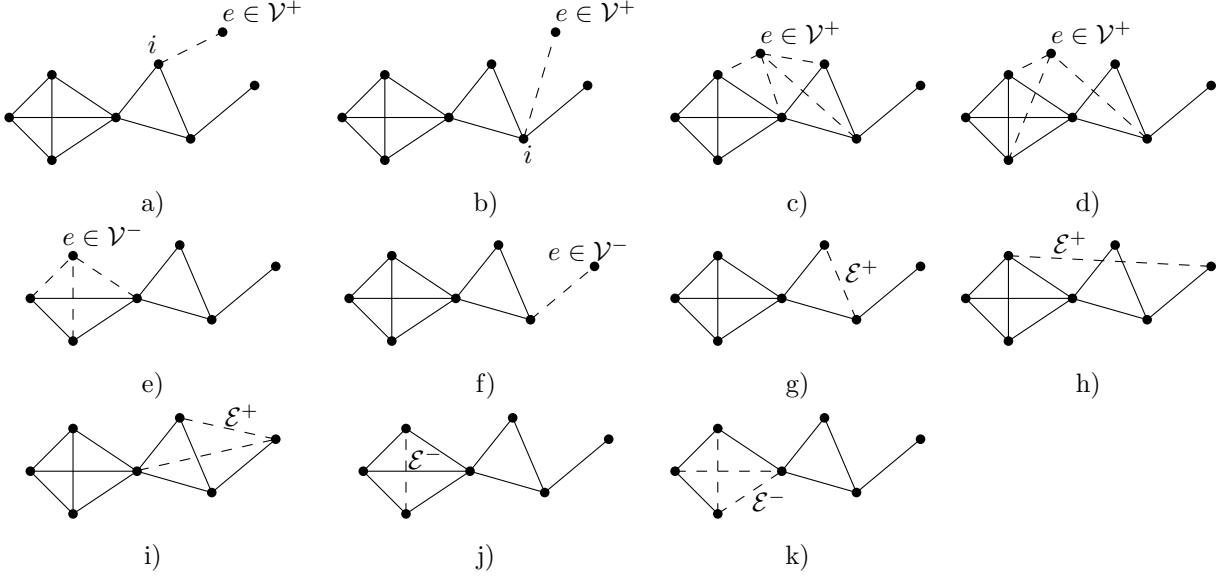


Fig. 4. Different possible changes over the graph: a) addition of a node, clique, and intersection; b) addition of a node, and clique; c) addition of a node to an existing clique; d) addition of a node with more than one edge (redundant links); e) removal of a node making a clique smaller; f) removal of a node disappearing both a clique and an intersection; g) addition of an edge merging two cliques; h) addition of an edge that does not modify the set of cliques; i) addition of more than one edge merging cliques; j) removal of an edge dividing a clique into more cliques and without adding intersection nodes; k) removal of more than one edge dividing a clique and including intersection nodes.

5.1 Addition of nodes

Let \mathcal{V}^+ be the set of new nodes added to the graph, i.e., the set of vertices is modified to be $\mathcal{V} \cup \mathcal{V}^+$. Suppose that the addition of the new nodes \mathcal{V}^+ are connected to a subset of already existing nodes denoted by $\hat{\mathcal{V}} \subset \mathcal{V}$. The addition of \mathcal{V}^+ is made throughout the set of edges denoted by $\mathcal{E}^+ = \{(i, j) : j \in \mathcal{V}^+, i \in \hat{\mathcal{V}} \subseteq \mathcal{V}\}$, i.e., the set of edges is modified to be $\mathcal{E} \cup \mathcal{E}^+$. Without loss of generality, let $|\mathcal{V}^+| = 1$, i.e., $\mathcal{V}^+ = \{e\}$. At this point, there are different possible cases to analyze, which depend on the cardinality of the set of new edges added to the graph, denoted by $|\hat{\mathcal{V}}|$.

5.1.1 Addition of $e \in \mathcal{V}^+$ throughout one edge ($|\hat{\mathcal{V}}| = 1$)

In this case, the addition of the node $e \in \mathcal{V}^+$ implies necessarily the addition of a new clique since it is included throughout only one edge. It is not possible that the node $e \in \mathcal{V}^+$ belongs to an already existing clique that is at least composed of two nodes. Then, there must be an addition of population dynamics. On the other hand, if $\hat{\mathcal{V}} \cap \mathcal{I} = \emptyset$, then the addition of the node $e \in \mathcal{V}^+$ implies that a node $i \in \hat{\mathcal{V}}$ becomes an intersection node (see Figure 4 a)). Consequently, this implies an addition of mass dynamics. In contrast, if $\hat{\mathcal{V}} \cap \mathcal{I} \neq \emptyset$, then the added edge $\mathcal{E}^+ = \{(e, i)\}$ connects the new node $e \in \mathcal{V}^+$ with an intersection node $i \in \mathcal{I}$, and it is not necessary to add new mass dynamics (see Figure 4 b)).

5.1.2 Addition of $e \in \mathcal{V}^+$ throughout more than one edge ($|\hat{\mathcal{V}}| > 1$)

When the new node $e \in \mathcal{V}^+$ is added throughout more than one edge, the addition does not necessarily imply the addition of a clique (otherwise, it implies a modification of an existing dynamics). In the case that $\mathcal{V}^p \subseteq \hat{\mathcal{V}}$, for any $p \in \mathcal{P}$, then the node $e \in \mathcal{V}^+$ becomes part of the clique \mathcal{C}^p and the dynamics associated to this population must be extended (see Figure 4 c)). Moreover, this case does not modify the mass dynamics in any sense. In contrast, if

$\mathcal{V}^p \notin \hat{\mathcal{V}}$, then the addition of $e \in \mathcal{V}^+$ must be treated as in Sub-section 5.1.1 and with $|\hat{\mathcal{V}}| - 1$ redundant links (see Figure 4 d)).

5.2 Removal of nodes

Let \mathcal{V}^- be the set of removed nodes from the graph, i.e., the set of vertices is modified to be $\mathcal{V} \setminus \mathcal{V}^-$. The removal of nodes \mathcal{V}^- implies the removal of all the edges associated to them, given by $\mathcal{E}^- = \{(i, j) : j \in \mathcal{V}^-, i \in \mathcal{V}\}$, i.e., the set of edges is modified to be $\mathcal{E} \setminus \mathcal{E}^-$. Without loss of generality, let $|\mathcal{V}^-| = 1$, i.e., $\mathcal{V}^- = \{e\}$. Notice that it is not possible to remove an intersection node since it would violate the assumption that \mathcal{G} is a connected graph, i.e., $e \notin \mathcal{I}$. Finally, the removal of a node $e \in \mathcal{V}^-$ implies the modification of the dynamics associated to the population $p \in \mathcal{P}_e$ (see Figure 4 e)).

Furthermore, suppose that there is a clique \mathcal{C}^p composed of two nodes $\mathcal{V}^p = \{i, e\}$ and only one intersection node denoted by $i \in \mathcal{I}^p$. When the node e is removed from the set of nodes \mathcal{V}^p , the clique \mathcal{C}^p also disappears and the node $i \in \mathcal{V}$ is not longer an intersection node, then one mass dynamics also disappear (see Figure 4 f)). Otherwise, the removal of nodes cannot affect mass dynamics.

5.3 Addition of edges

First, due to the fact that the set of nodes remains the same as the set of already existing edges, then the addition of edges does not imply a change in the dynamics already designed. However, the addition of edges might allow the reduction of cliques. Consequently, the addition of edges might allow the reduction of the number of population dynamics. Moreover, *the mentioned reduction is not required for the system to keep converging towards the solution.*

Let \mathcal{E}^+ be the set of edges added to the graph, i.e., the set of edges is modified to be $\mathcal{E} \cup \mathcal{E}^+$. In general, the addition of edges cannot imply the addition of cliques, but could imply the reduction of the optimal set of cliques, i.e., the addition of edges might merge different cliques into one complete graph.

5.3.1 Addition of one edge ($|\mathcal{E}^+| = 1$)

The edge is characterized by $\mathcal{E}^+ = \{(i, j) : i \in \mathcal{V}^p, j \in \mathcal{V}^q\}$, where $p, q \in \mathcal{P}$. Notice that i and j cannot belong to the same clique (each clique is a complete graph). If for those two populations $p \neq q$, $\mathcal{I}^p \cap \mathcal{I}^q \neq \emptyset$, and $|\mathcal{V}^p| = |\mathcal{V}^q| = 2$, then there is a reduction of cliques. The new clique is given by the set of vertices $\mathcal{V}^p \cup \mathcal{V}^q$ and the set of edges $\mathcal{E}^p \cup \mathcal{E}^q \cup \mathcal{E}^+$ (see Figure 4 g)). This situation implies the modification of an intersection node, and the modification of the population dynamics associated to populations $p, q \in \mathcal{P}$ into unified population dynamics.

Moreover, this case is a quite particular one that requires the existence of two cliques of two nodes each one. Any different case for the added edge \mathcal{E}^+ is a redundant link and does not imply any modification, neither over the population dynamics nor over the mass dynamics. For instance, if there are not cliques composed of only two nodes, any addition of an edge might be ignored straightforward as a redundant link (see Figure 4 h)).

5.3.2 Addition of more one edge ($|\mathcal{E}^+| > 1$)

When adding more than one edge, it is possible to obtain a reduction of cliques within the graph that describes the social topology, i.e., it is possible that two or more populations merge into only one population. In order to analyze the addition of more than one edge, consider the set of new edges denoted by $\mathcal{E}^+ = \{(i, j) : i, j \in \hat{\mathcal{V}}\}$. For simplicity, and without loss of generality, suppose that two cliques \mathcal{C}^p , and \mathcal{C}^q , corresponding to populations $p, q \in \mathcal{P}$, share an intersection node $e \in \mathcal{I}$, i.e., $e \in (\mathcal{I}^p \cap \mathcal{I}^q)$. Then, the only possibility of having a reduction within a clique is that the addition of edges is given by $\mathcal{E}^+ = \{(i, j), \text{ for all } i \in \hat{\mathcal{V}}^p, \text{ and } j \in \hat{\mathcal{V}}^q\}$, where $\hat{\mathcal{V}}^p = \mathcal{V}^p \setminus \{e\}$, and $\hat{\mathcal{V}}^q = \mathcal{V}^q \setminus \{e\}$. This fact implies that cliques \mathcal{C}^p , and \mathcal{C}^q become the same clique whose set of vertices is given by $\mathcal{V}^p \cup \mathcal{V}^q$ and whose set of edges is given by $\mathcal{E}^p \cup \mathcal{E}^q \cup \mathcal{E}^+$ (see Figure 4 i)).

5.4 Removal of edges

The removal of edges in an optimal set of cliques necessarily implies the addition of the number of cliques, i.e., an edge is removed from a complete graph, making it split into more sub-complete graphs composing new and smaller cliques. Moreover, the removal of edges might cause that a node becomes an intersection node.

Let $\mathcal{E}^- = \{(i, j) : i, j \in \hat{\mathcal{V}} \subset \mathcal{V}^p\}$ be the set of edges that are removed from a clique associated to a population $p \in \mathcal{P}$. Notice that the less amount of edges implies the splitting of the clique into two cliques, and several edges might become redundant (see Figure 4 j)). On the other hand, the complete graph for the population $p \in \mathcal{P}$ is composed of $(|\mathcal{V}^p|(|\mathcal{V}^p| - 1))/2$ edges. Consequently, the larger amount of edges that might be removed from a clique is given by $(|\mathcal{V}^p|^2 - 3|\mathcal{V}^p| + 2)/2$, generating $|\mathcal{V}^p| - 2$ extra populations, and then intersection nodes appear in the social topology, i.e., one population dynamics should be modified, $|\mathcal{V}^p| - 2$ extra population dynamics should be included, and $|\mathcal{V}^p| - 2$ mass dynamics should be added (see Figure 4 k)).

6 Optimization problems with constraints

One of the main features of full potential games is that their Nash equilibrium points coincide with the extreme points of the corresponding potential function, i.e., Nash equilibria satisfy the KKT first-order conditions [23]. Additionally, if the potential function is concave, potential games are stable and an optimization problem can be solved in a distributed way by using the population dynamics and the mass dynamics shown in Section 3. Some optimization problem forms are set in this section, and illustrative examples are solved with the population and mass dynamics presented previously. First, we consider the classical optimization problem of a population game, i.e., an optimization problem with a constraint given by the positiveness of the proportion of agents and the constraint given by the social mass. Afterwards, we consider an optimization problem of a population game without a constraint given by the social mass. The last mentioned optimization problem allows to illustrate how trajectories of fitness functions can be forced to converge to a desired value. Finally, the fact that trajectories may be forced towards a desired value allows to extend the consideration of constraints.

6.1 Optimization problem with social mass constraint

The general optimization problem related to population dynamics with full potential games is presented next. This problem is a resource allocation problem, where m is the total resource amount. The problem is stated as

$$\begin{aligned} & \underset{\mathbf{x}}{\text{maximize}} && f(\mathbf{x}) \\ & \text{subject to} && \sum_{i=1}^N x_i = m, \text{ and } \mathbf{x} \in \mathbb{R}_+^N, \end{aligned}$$

where $f : \mathbb{R}_+^N \mapsto \mathbb{R}$ and $m \in \mathbb{R}_+$. It is assumed that f is continuously differentiable and concave. Then, there is a full potential stable game given by $\mathbf{F}(\mathbf{x}) = \nabla f(\mathbf{x})$.

The first constraint in this optimization problem determines the set of social states $\mathbf{x} \in \Delta$, and the second constraint is satisfied with population dynamics since the states are defined to be positive. Constraints about information availability are given by a graph, which determines possible dependency among populations.

Example 6.1.1 An academic example for this optimization problem is proposed as

$$\begin{aligned} & \underset{\mathbf{x}}{\text{maximize}} && -\mathbf{x}^\top \mathbf{W} \mathbf{x} + \mathbf{w}^\top \mathbf{x} \\ & \text{subject to} && \sum_{i=1}^{20} x_i = 250, \text{ and } \mathbf{x} \in \mathbb{R}_+^{20}, \end{aligned}$$

where $\mathbf{W} \in \mathbb{R}^{20 \times 20}$ is a sparse matrix with unitary diagonal and the entry $[\mathbf{W}]_{i,j} = 1$ for $(i, j) = (3, 13)$, and $\mathbf{w} \in \mathbb{R}^{20}$, $\mathbf{w} = [2 \ 4 \ 6 \ 8 \ 10 \ \dots \ 30 \ 32 \ 34 \ 36 \ 38 \ 40]^\top$. For this optimization problem, there are limitations in information dependency given by the graph shown in Figure 5 omitting the nodes named μ_1 , μ_2 , and r . The intersection nodes form a complete graph for which $\sum_{i \in \mathcal{I}} \kappa_i = m$ is guaranteed.

Convergence results are shown in Figures 7a) and 7c). It can be seen that the constraint related to social mass is satisfied, even when population masses vary over time. Also, since dynamics are defined only for positive variables then the additional constraint related to positiveness of the decision variable is satisfied as well. \square

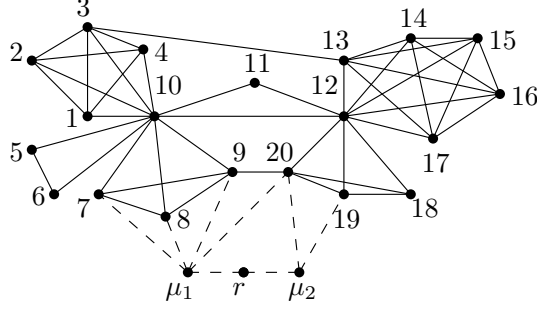


Fig. 5. Social topology with six populations and two intersection nodes.

Example 6.1.2 Consider the optimization problem given by

$$\begin{aligned} & \underset{\mathbf{x}}{\text{maximize}} && -\mathbf{x}^\top \mathbf{x} + \mathbf{w}^\top \mathbf{x} \\ & \text{subject to} && \sum_{i=1}^9 x_i = 100, \text{ and } \mathbf{x} \in \mathbb{R}_+^9, \end{aligned}$$

where $\mathbf{w} \in \mathbb{R}^9$, $\mathbf{w} = [20 \ 4 \ 6 \ 8 \ 10 \ 12 \ 14 \ 16 \ 18]^\top$. Suppose that, for this optimization problem, there are limitations over the information dependency given by the graph shown in Figure 6. Notice that the intersection nodes do not form a complete graph. Consequently, an auxiliary distributed population dynamics are proposed with the constraint $\sum_{i \in \mathcal{I}} \kappa_i = m$, equivalent to a simplex for a game including only intersection nodes [22]. Fitness functions do not vary for this auxiliary distributed problem.

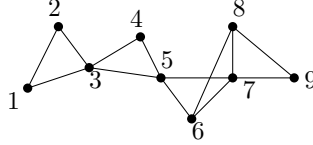


Fig. 6. Social topology with four populations and three intersection nodes.

The results of convergence are shown in Figures 7b) and 7d). It can be seen that the constraints related to social mass and positiveness of decision variables are satisfied. \square

6.2 Optimization problems without social mass constraint

A less restrictive optimization problem is studied. This problem only demands the positiveness of optimization variables. From a mass dynamics perspective, it implies a variation of the social mass arbitrarily. The problem is stated as follows:

$$\begin{aligned} & \underset{\mathbf{x}}{\text{maximize}} && f(\mathbf{x}) \\ & \text{subject to} && \mathbf{x} \in \mathbb{R}_+^N, \end{aligned}$$

where $f : \mathbb{R}_+^N \mapsto \mathbb{R}$, and f is continuously differentiable and concave. Also, it is supposed that the solution point of this problem is an interior point.

The solution for the optimization problem with one constraint is found by $\mathbf{F}(\mathbf{x}) = \nabla f(\mathbf{x}) = 0$, since $f(\mathbf{x})$ is concave and by the fact that it is known that the maximum point is an interior point. Therefore, the desired value for the average fitness is $F_i(r) = 0$, and it is enough to find the correct value for reference r and any intersection $i \in \mathcal{I}$.

Example 6.2.1 An academic example for this optimization problem is proposed as

$$\begin{aligned} & \underset{\mathbf{x}}{\text{maximize}} && -\mathbf{x}^\top \mathbf{W} \mathbf{x} + \mathbf{w}^\top \mathbf{x} \\ & \text{subject to} && \mathbf{x} \in \mathbb{R}_+^{20}, \end{aligned}$$

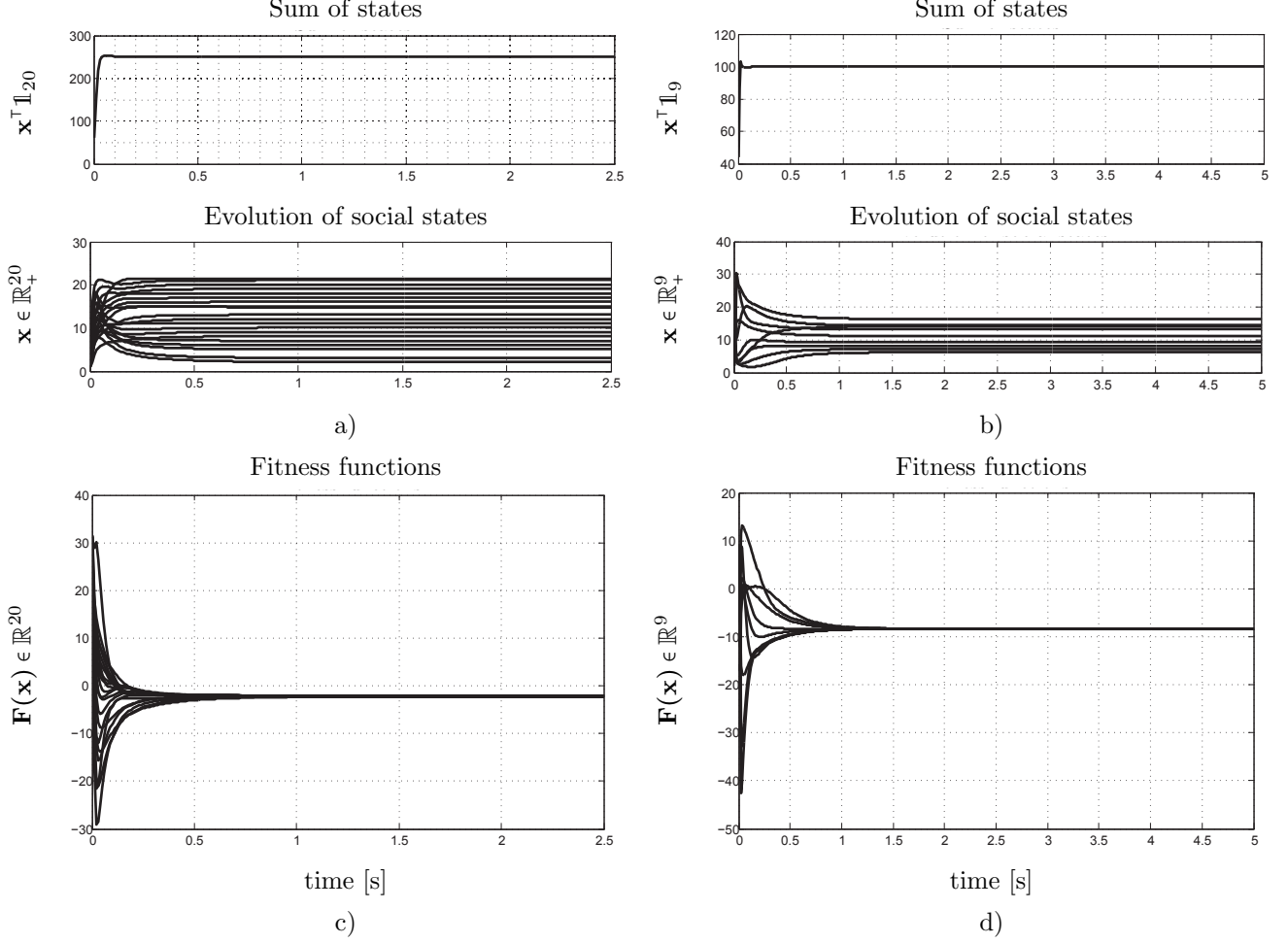


Fig. 7. Evolution of states and fitness functions.

where $\mathbf{W} \in \mathbb{R}^{20 \times 20}$ is a sparse matrix with unitary diagonal and entries $[\mathbf{W}]_{i,j} = 1$ for $(i,j) = \{(3,13), (9,20)\}$, and $\mathbf{w} \in \mathbb{R}^{20}$, $\mathbf{w} = [2 \ 4 \ 6 \ 8 \ 10 \ \dots \ 30 \ 32 \ 34 \ 36 \ 38 \ 40]^\top$. For this optimization problem, there are limitations over the information dependency given by the graph shown in Figure 5, omitting the nodes named μ_1 , μ_2 , and r .

Convergence results are shown in Figures 8a) and 8b), where it can be seen that the constraints related to positiveness are satisfied. \square

6.3 Optimization problems with multiple constraints over agents proportions

Suppose that there is a strategic interaction with more than one constraint, e.g., different constraints over the proportion of agents. It is desired that the total amount of certain groups of proportions of agents are constant. This problem is stated as

$$\begin{aligned} & \underset{\mathbf{x}}{\text{maximize}} && f(\mathbf{x}) \\ & \text{subject to} && \mathbf{H}\mathbf{x} = \mathbf{h}, \text{ and } \mathbf{x} \in \mathbb{R}_+^N, \end{aligned} \quad (14)$$

where $\mathbf{x} \in \mathbb{R}_+^N$, $f: \mathbb{R}_+^N \mapsto \mathbb{R}$, and f is concave and continuously differentiable. Moreover, $\mathbf{H} \in \mathbb{R}^{L \times N}$ since there are L constraints and N decision variables, and $\mathbf{h} \in \mathbb{R}^L$. For this optimization problem, μ is the Lagrange multiplier vector. The Lagrange function $l: \mathbb{R}^N \times \mathbb{R}^L \mapsto \mathbb{R}$ is

$$l(\mathbf{x}, \mu) = f(\mathbf{x}) + \mu^\top (\mathbf{H}\mathbf{x} - \mathbf{h}). \quad (15)$$

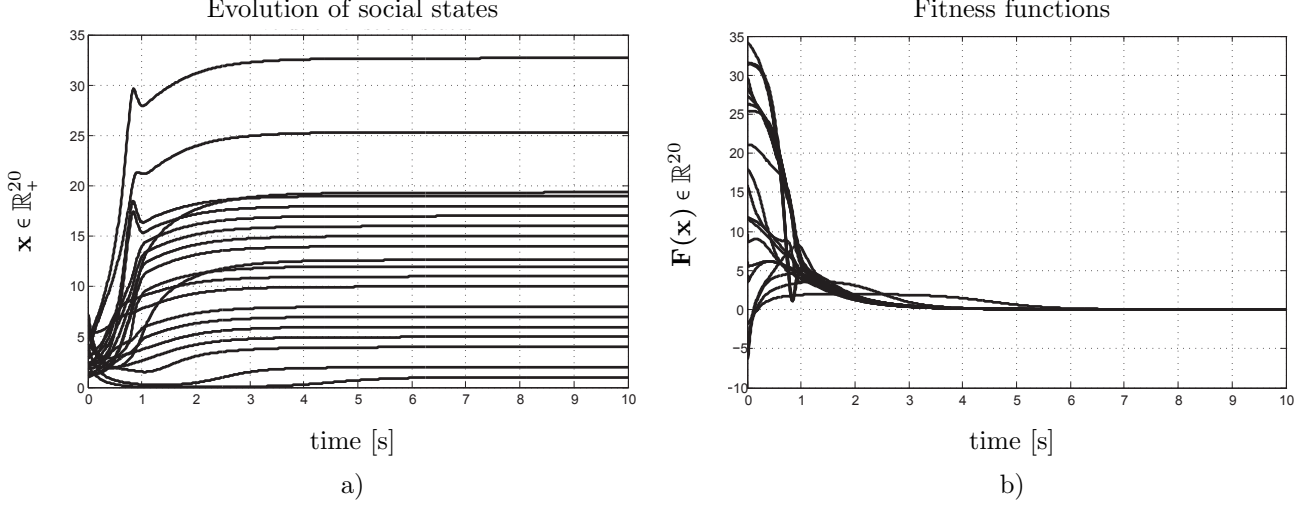


Fig. 8. Evolution of states and fitness functions.

Moreover, $\nabla_{\mathbf{x}}l(\mathbf{x}, \mu) = \nabla f(\mathbf{x}) + \mathbf{H}^\top \mu$, and $-\nabla_{\mu}l(\mathbf{x}, \mu) = -\mathbf{H}\mathbf{x} + \mathbf{h}$. The Lagrange condition is used to find possible extreme points in the objective function, in which $\nabla_{\mathbf{x}}l(\mathbf{x}, \mu) = 0$, $\nabla_{\mu}l(\mathbf{x}, \mu) = 0$.

Consequently, fitness functions for each node are chosen to be defined as $\mathbf{F}(\mathbf{x}) = \nabla_{\mathbf{x}}l(\mathbf{x}, \mu)$, and $\mathbf{F}(\mu) = \nabla_{\mu}l(\mathbf{x}, \mu)$. This problem is solved by using a reference r as it was explained in Sub-section 3.3 in order to force a convergence value for the fitness functions associated to the social states and the Lagrange multipliers. For both $\mathbf{F}(\mathbf{x})$ and $\mathbf{F}(\mu)$, a fictitious function can be set as explained in Remark 2. In order to use the population and the mass dynamics, it is necessary that the games are stable according to Assumption 3.

Lemma 2 *If $f(\mathbf{x})$ is twice continuously differentiable and concave, and the constraints have the form $\mathbf{H}\mathbf{x} = \mathbf{h}$, then the games $\mathbf{F}(\mathbf{x}) = \nabla_{\mathbf{x}}l(\mathbf{x}, \mu)$ and $\mathbf{F}(\mu) = \nabla_{\mu}l(\mathbf{x}, \mu)$ are stable.*

PROOF. The Lagrangian function is defined as in (15), and the fitness functions are given by $\mathbf{F}(\mathbf{x}) = \nabla f(\mathbf{x}) + \mathbf{H}^\top \mu$, $\mathbf{F}(\mu) = -\mathbf{H}\mathbf{x} + \mathbf{h}$.

The derivative of $\mathbf{F}(\mathbf{x})$ with respect to \mathbf{x} is $D_{\mathbf{x}}\mathbf{F}(\mathbf{x}) = \nabla^2 f(\mathbf{x})$, that is the Hessian matrix $\mathbf{J} \leq 0$ since $f(\mathbf{x})$ is concave. The derivative of $\mathbf{F}(\mu)$ with respect to μ is $D_{\mu}\mathbf{F}(\mu) = 0$. Therefore $\mathbf{F}(\mathbf{x})$ and $\mathbf{F}(\mu)$ are stable games. ■

Remark 4 *Notice that the optimization problems with constraints of the form $\mathbf{P}\mathbf{x} \leq \mathbf{p}$ can be written as the form $\mathbf{H}\mathbf{x} = \mathbf{h}$ by using slack variables.* ◇

Example 6.3.1 An academic example for this optimization problem is proposed as follows:

$$\begin{aligned}
 & \underset{\mathbf{x}}{\text{maximize}} && -\mathbf{x}^\top \mathbf{x} + \mathbf{w}^\top \mathbf{x} \\
 & \text{subject to} && x_7 + x_8 + x_9 + x_{20} = \mathbf{x}_{c1}^\top \mathbf{1}_{[4]} = 25 \\
 & && x_{18} + x_{19} + x_{20} = \mathbf{x}_{c2}^\top \mathbf{1}_{[3]} = 15 \\
 & && x \in \mathbb{R}_+^{20},
 \end{aligned}$$

where $\mathbf{w} \in \mathbb{R}^{20}$, $\mathbf{w} = [11 \ 13 \ 12 \ 9 \ 6 \ 7 \ 8 \ 15 \ 14 \ 9.5 \ 10.5 \ 11.5 \ 12.5 \ 18 \ 17 \ 16 \ 5 \ 20 \ 4 \ 2]^\top$, $\mathbf{x}_{c1} = [x_7 \ x_8 \ x_9 \ x_{20}]^\top$, and $\mathbf{x}_{c2} = [x_{18} \ x_{19} \ x_{20}]^\top$. For this optimization problem, there are limitations in information dependency given by the graph shown in Figure 5 including the nodes named μ_1 and μ_2 , which are the Lagrange multipliers associated to the constraints.

The convergence of the population states towards the solution can be seen in Figure 9a), and the convergence of fitness functions is shown in Figure 9b). Results show that there is a transitory event in which trajectories do not belong to the feasible region. However, the population and the mass dynamics force the trajectories to converge to

the solution despite this fact. The convergence to the feasible region could be faster by increasing the convergence factor β . \square

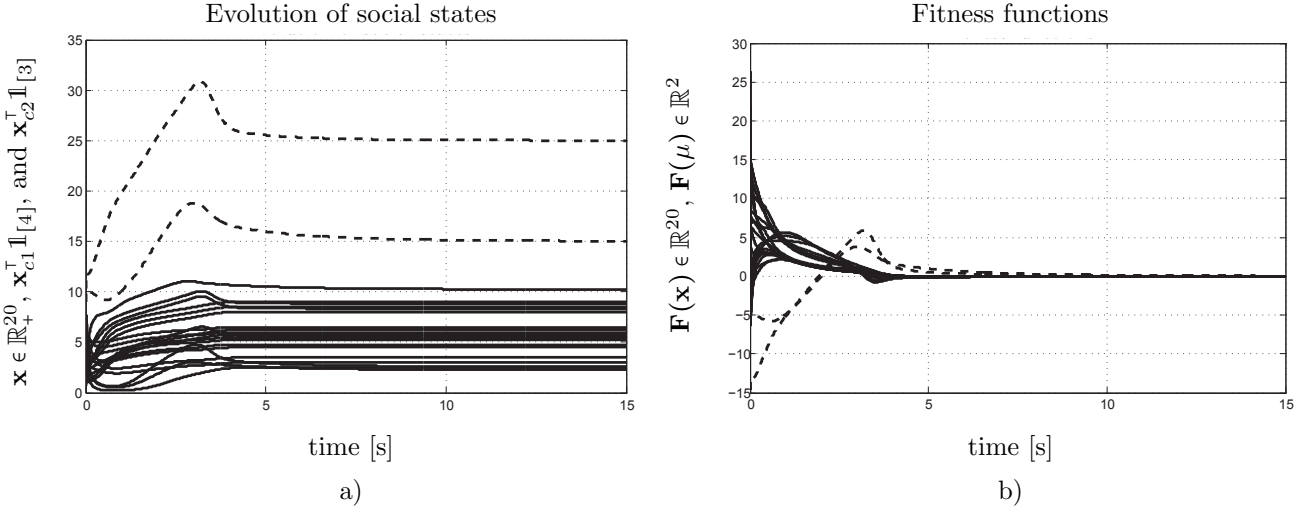


Fig. 9. Evolution of states and fitness functions.

7 Performance against disturbances and the convergence factor

As it has been shown in Section 3, the convergence factor β forces trajectories towards the feasible region. This fact makes the proposed methodology robust against disturbances. In order to illustrate this feature, Example 6.1.1 is solved under different conditions. First, the initial condition does not belong to the feasible region (i.e., $\mathbf{x}(0) \notin \Delta$). Additionally, as a second factor affecting the evolution of states, a hard disturbance is applied to a node in the graph shown in Figure 5. The disturbance can be applied to any arbitrary node (or to more than one node (state)). However, disturbances in an intersection node have more repercussions over the total society, i.e., the disturbance over the proportion of agents of an intersection node $i \in \mathcal{I}$ affects all the proportion of agents x_j^p for all $j \in \mathcal{S}^p$, and for all the populations $p \in \mathcal{P}_i$, and consequently all the trajectories leave the simplex sets Δ^p for all $p \in \mathcal{P}_i$.

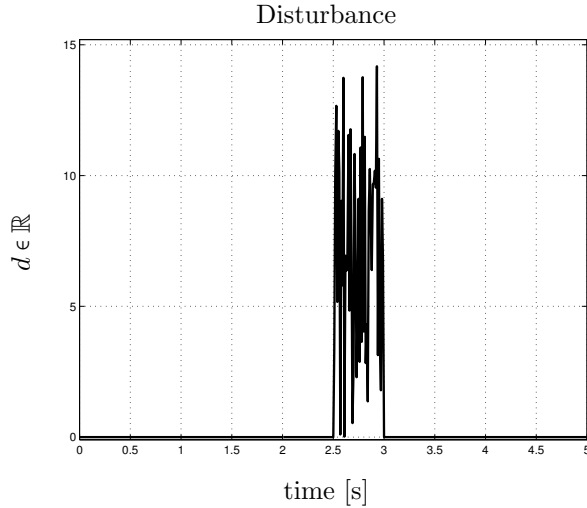


Fig. 10. Abrupt disturbance at intersection node $10 \in \mathcal{I}$ (i.e., affecting state x_{10} , and all the proportion within the populations $p \in \mathcal{P}_{10}$).

In this case, the intersection node $10 \in \mathcal{V}$ is selected such that many other nodes are affected in the graph because of the direct connectivity with it, representing disturbances on $10 \in \mathcal{V}$ a critical situation. Figure 10 shows the disturbance $d \in \mathbb{R}$ with an amplitude of about 15 applied to the intersection node. That disturbance is applied to

the proportion of agents corresponding to the node, i.e., x_{10}^p , for all $p \in \mathcal{P}_{10}$. Then, d affects the fitness functions \mathbf{F}^p , and it also affects the evolution of the population masses m^p , for all $p \in \mathcal{P}_{10}$. Moreover, the disturbance pushes the proportion of agents trajectories away from the feasible region since it affects the total sum of proportions. We illustrate that the elements ϕ^p in (6a) for all $p \in \mathcal{P}$, and ψ_i in (7a) for all $i \in \mathcal{I}$, maintain the proportion of agents evolving to the corresponding feasible region.

Figure 11 shows the evolution of the states and the fitness functions for two different values of β . Figure 11a) and 11c) show results for $\beta = 10$. It can be seen that the trajectories of states take around 1.5 s to satisfy the constraint, then, trajectories get out the feasible region because of the applied disturbance and trajectories return to feasible region at $t = 3.5$ s. On the other hand, Figures 11b) and 11d) show results for a larger convergence factor $\beta = 1000$. It can be seen a fast convergence to the feasible region at the beginning of the states evolution, and then after disturbance, almost an immediate evolution towards the feasible region is newly obtained. Finally, it is necessary to point out that this shown behavior against disturbances occurs for any of the optimization problems presented in Section 6.

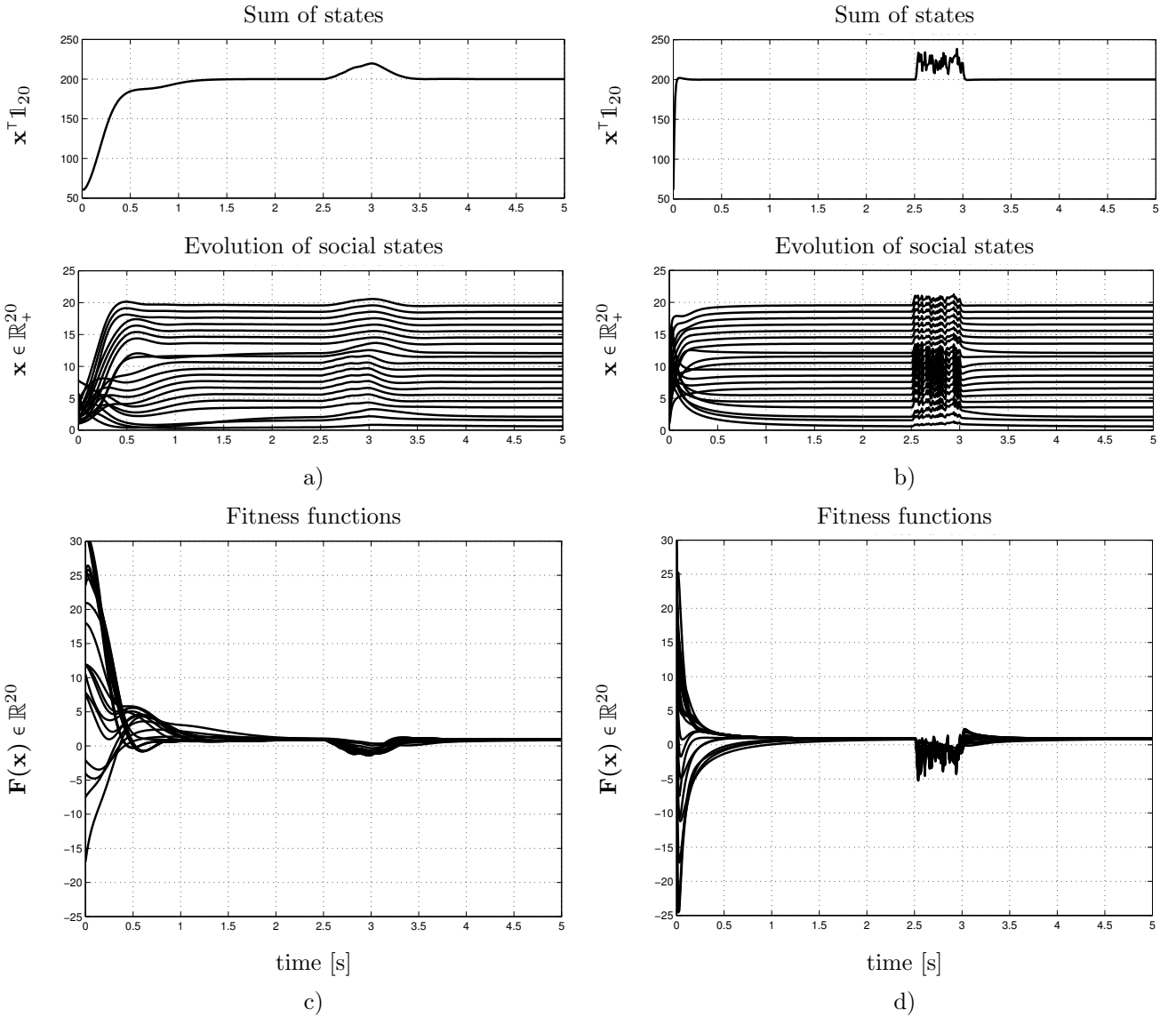


Fig. 11. Evolution of states and fitness functions with initial condition $\mathbf{x}(0) \notin \Delta$, and with disturbance on an intersection node.

8 Case study

In an optimal control design, the control actions are commonly the decision variables. Then, from the point of view of our proposed approach, the proportion of agents playing each strategy is associated to each control action of the system. It is guaranteed that the solution obtained with the proposed approach satisfies the established constraints. However, due to the fact that trajectories of proportion of agents might get out from the feasible region in a transitory event, it is not convenient to apply these proportions as the control actions in a continuous time. For this reason, we present the design of a controller based on the population and mass dynamics for a discrete-time system.

The Barcelona Drinking Water Network (BDWN) is a large-scale system managed by *Aguas de Barcelona S.A.* (AGBAR). The network is mainly composed of tanks, valves, pumps, drinking water sources, and water demands [20,21]. The volume at tanks is represented by a state vector denoted by $\mathbf{v} \in \mathbb{R}_+^{N_v}$, the flows through the valves and pumps are represented by the control actions vector denoted by $\mathbf{u} \in \mathbb{R}^{N_x}$, and the water-demanded flows are represented by the disturbance vector $\mathbf{d} \in \mathbb{R}^{N_d}$. The corresponding discrete-time model with sampling time $\Delta t = 1$ hour is given by

$$\mathbf{v}(k+1) = \mathbf{A}\mathbf{v}(k) + \mathbf{B}\mathbf{u}(k) + \mathbf{B}_l\mathbf{d}(k), \quad (16a)$$

$$\mathbf{0} = \mathbf{E}_x\mathbf{u}(k) + \mathbf{E}_d\mathbf{d}(k), \quad (16b)$$

where $k \in \mathbb{Z}_+$ denotes the discrete time. The difference equation in (16a) describes the dynamics of the storage tanks, and (16b) describes the static relations given by the mass balance at the junction nodes. Moreover, $\mathbf{0}$ is a column vector of null entries with suitable dimensions, and \mathbf{A} , \mathbf{B} , \mathbf{B}_l , \mathbf{E}_x , and \mathbf{E}_d are constant matrices with suitable dimensions.

Remark 5 *The evolution of the proportion of agents converging to a solution is given in continuous time, i.e., $\mathbf{x}(t)$, whereas the control action sequence is given in discrete time, i.e., $\mathbf{u}(k)$. At each iteration, a population game is solved to compute the proper control action. Moreover, if the initial condition for the proportion of agents associated to the control actions is given by $\mathbf{x}(0) = \mathbf{u}(k)$, then the control action applied to the system in the next iteration is defined as $\mathbf{u}(k+1) \triangleq \mathbf{x}(\Delta t) = \mathbf{x}^*$ of the k^{th} population game (there is a population game at each iteration). Notice that the population game should converge towards its solution in a time shorter than Δt (for the presented case study, $\Delta t = 1$ hour, which is more than enough time to converge towards the solution \mathbf{x}^*). From now on, the control action $\mathbf{u}(k)$ is denoted by $\mathbf{x}(k)$, in order to relate it directly to the proportion of agents in the population game. \diamond*

The BDWN is shown in Figure 12. The social topology, given by the information network is going to be discussed later in Section 8.1, has 61 available strategies associated to the control actions. Equation (16b) summarizes the constraints presented in Table 1. It is also important to point out that the system shown in Figure 12 has 11 nodes corresponding to the mass-balance constraints and which should not be confused to the edges in the social topology graph.

Table 1
Node constraints

Node	Constraint	Node	Constraint
1	$x_1 - x_2 - x_5 - x_6 = 0$	7	$x_{25} - x_{26} + x_{32} + x_{34} + x_{40} - x_{41} = d_{15}$
2	$x_2 - x_3 = d_2$	8	$x_{39} - x_{45} + x_{46} - x_{47} = d_{17}$
3	$-x_{13} + x_{18} = d_5$	9	$x_{28} - x_{35} - x_{43} + x_{49} = d_{16}$
4	$x_{14} + x_{15} - x_{19} - x_{25} + x_{26} = d_7$	10	$x_{43} + x_{44} + x_{52} = d_{20}$
5	$x_{22} - x_{30} = d_9$	11	$-x_{50} - x_{51} - x_{52} - x_{56} - x_{57} - x_{58} - x_{59} - x_{60} + x_{61} = d_{25}$
6	$x_{31} - x_{39} - x_{40} = d_{14}$		

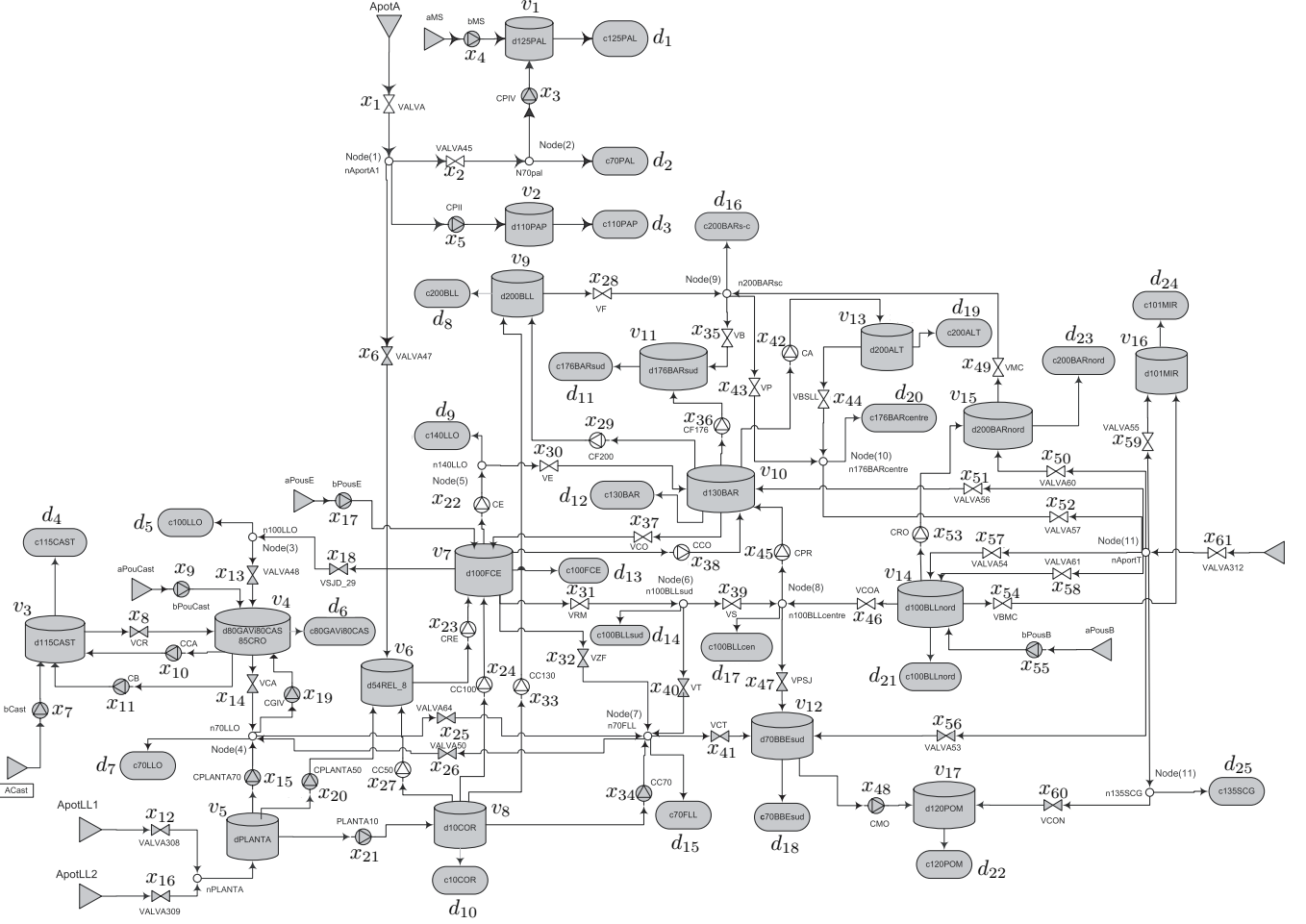


Fig. 12. Aggregate model of the Barcelona Drinking Water Network (BDWN), comprised by 17 states, 61 control actions, 25 demands, and 11 mass-balance nodes.

8.1 Partitioning of the network

Partitioning of the BDWN is a problem already studied in [19]. For the BDWN control problem, the proposed partitioning is determined based on the system mass-balance constraints. As in Section 6, Lagrange-multiplier vertices are connected to decision variables vertices from which information is needed in order to compute the fitness functions $\mathbf{F}(\mu)$. As a criterion for performing the partitioning, it is desired that all the Lagrange multipliers, and the nodes connected with them, belong to the same clique. In order to formalize this partitioning criterion, let \mathcal{H}_j be the set of all the nodes that are involved in the j^{th} equality constraint of the form (14), where $j = 1, \dots, L$, e.g., for the BDWN system, $\mathcal{H}_1 = \{1, 2, 5, 6\}$, and $\mathcal{H}_2 = \{2, 3\}$. Furthermore, we consider two sets of nodes for mass-balance constraints \mathcal{H}_i , and \mathcal{H}_j . If $\mathcal{H}_i \cap \mathcal{H}_j \neq \emptyset$, then all the nodes $\mathcal{H}_i \cup \mathcal{H}_j$ should belong to the same clique.

Based on this idea, it is possible to determine the vertices (strategies) that should belong to the same clique (population). As an example, consider the set of nodes associated to the constraint given by mass-balance node 9, i.e., $\mathcal{H}_9 = \{28, 35, 43, 49\}$, and the set of nodes corresponding to the mass-balance constraint 10, i.e., $\mathcal{H}_{10} = \{43, 44, 52\}$. There is a common vertex given by $\mathcal{H}_9 \cap \mathcal{H}_{10} = \{43\}$. Now, considering the constraint corresponding to the mass-balance node 11, i.e., $\mathcal{H}_{11} = \{50, 51, 52, 56, 57, 58, 59, 60, 61\}$, then it is obtained that $\mathcal{H}_{10} \cap \mathcal{H}_{11} = \{52\}$. Consequently, there is a clique including all elements involved in mass-balance constraints 9, 10, and 11 from Table 1, i.e., all the nodes $\mathcal{H}_9 \cup \mathcal{H}_{10} \cup \mathcal{H}_{11}$ should belong to the same clique.

On the other hand, there are some vertices that are not associated to any constraint, e.g., the node 4 associated to the decision variable x_4 , then $4 \notin \mathcal{H}_j$ for all $j = 1, \dots, 11$. In these cases, vertices are assigned to the closest clique. Cliques

are presented in Figure 13, and the nodes of each clique are shown in Table 2. Notice that $\{\mathcal{H}_1 \cup \mathcal{H}_2 \cup \mathcal{H}_3 \cup \mathcal{H}_5\} \in \mathcal{V}^1$, $\{\mathcal{H}_4 \cup \mathcal{H}_6 \cup \mathcal{H}_7 \cup \mathcal{H}_8\} \in \mathcal{V}^2$, and $\{\mathcal{H}_9 \cup \mathcal{H}_{10} \cup \mathcal{H}_{11}\} \in \mathcal{V}^3$.

Table 2
Partitioning of the network into the three resultant cliques.

Clique	Vertices x	Involved states v
1	1, 2, 3, 4, 5, 6, 7, 8, 9, 10, 11, 13, 17, 18, 22, 29, 30, 36, 37, 38	1, 2, 3, 4, 6, 7, 9, 10, 11
2	12, 14, 15, 16, 19, 20, 21, 23, 24, 25, 26, 27, 31, 32, 33, 34, 39, 40, 41, 45, 46, 47	4, 5, 6, 7, 8, 9, 10, 12, 14
3	28, 35, 42, 43, 44, 48, 49, 50, 51, 52, 53, 54, 55, 56, 57, 58, 59, 60, 61	9, 10, 11, 12, 13, 14, 15, 16, 17

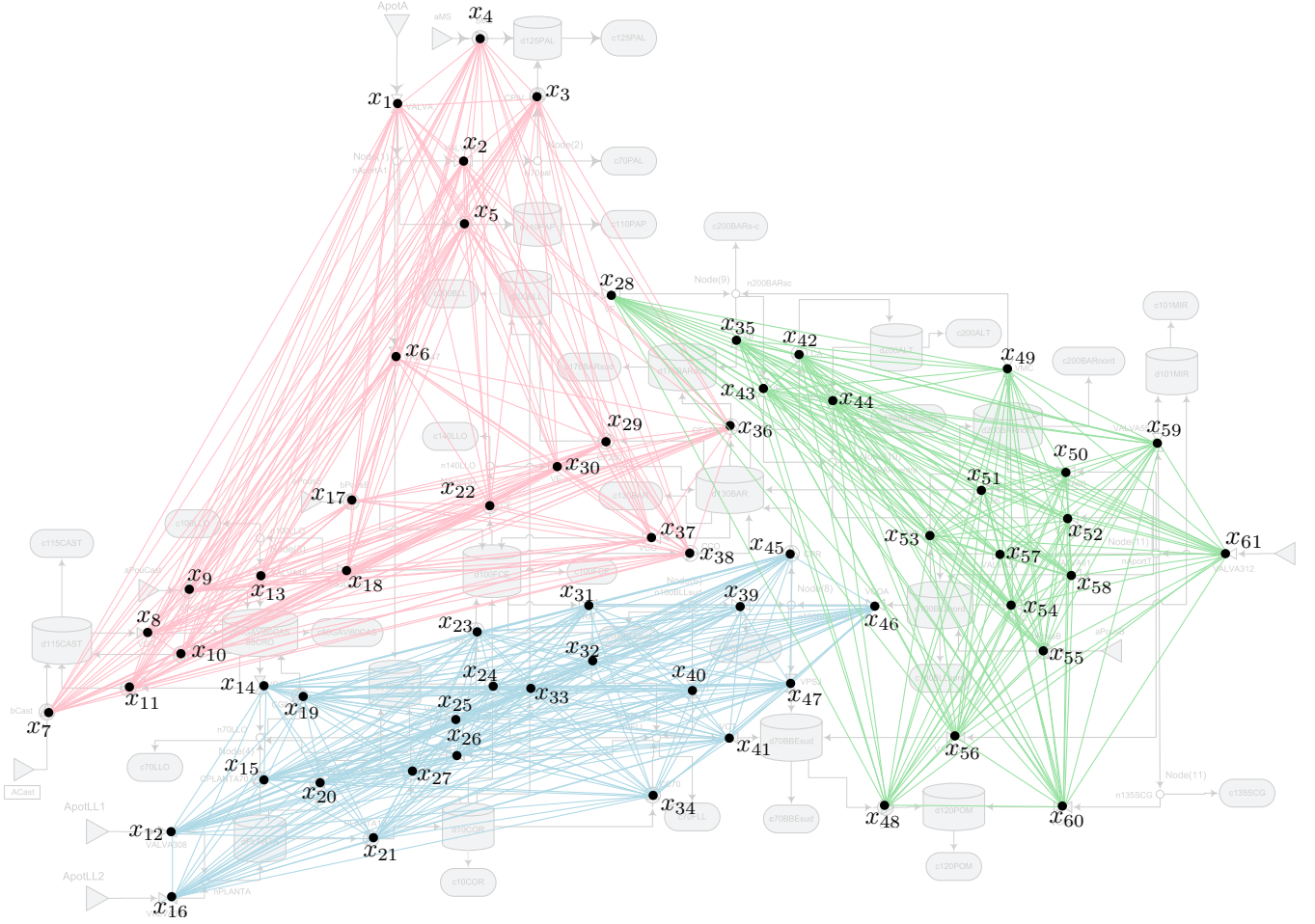


Fig. 13. Partitioning of the BDWN into three cliques (see Table 2).

8.2 System management criteria

The desired control performance is described by operational control objectives, which are determined by the company in charge of the management of the network. There are three main objectives, i.e., *i*) economic operation, *ii*) safety operation, and *iii*) smooth operation. Regarding the economical aspect, there are two costs, one of them associated to the water cost, and the other one associated to the energy costs to operate the network actuators (mainly pumping stations). The energy costs vary over time. These mentioned costs are denoted by $\alpha_1 \in \mathbb{R}^{N_x}$, and $\alpha_2(k) \in \mathbb{R}^{N_x}$, respectively. The economic operation objective is to minimize both the water production costs and the transportation

costs given in economic units² (e.u.), i.e.,

$$f_1(\mathbf{x}(k)) = (\alpha_1 + \alpha_2(k))^\top \mathbf{x}(k).$$

Regarding the safety operation, the objective consists in guaranteeing that there is enough stored water to satisfy the demands within the network, given by a safety volume denoted by $\mathbf{v}_s \in \mathbb{R}^{N_v}$. This objective is managed through the following soft constraint [7]:

$$\mathbf{v}(k) \geq \mathbf{v}_s - \boldsymbol{\xi}(k).$$

Moreover, it is desired that $\boldsymbol{\xi} \in \mathbb{R}^{N_v}$ tends to zero in order to make the tank volume be greater than the safety value. Consequently, the objective associated to the safety operation is given by

$$f_2(\boldsymbol{\xi}(k)) = \boldsymbol{\xi}(k)^\top \boldsymbol{\xi}(k).$$

Finally, as a third objective, it is desired to guarantee a smooth operation of the control devices, i.e., to penalize the variations of the control actions along the time given by $\Delta \mathbf{x}(k) = \mathbf{x}(k) - \mathbf{x}(k-1)$. This objective consists in minimizing

$$f_3(\mathbf{x}(k)) = \Delta \mathbf{x}(k)^\top \Delta \mathbf{x}(k).$$

The most important objective is the economical aspect, the second priority within the objectives is the safety operation, and the less important objective is the smooth operation.

8.3 Control design

In general, the design of a controller by using a population dynamics approach consists in the design of the fitness functions. In this paper, the design of the controllers with the proposed populations and mass dynamics consists in developing the statement of an optimization problem into a convenient form. Then, the fitness function can be established as well as the design of both the population and mass dynamics. In this section, two controllers are designed by using the proposed approach. First, the cost function is composed of the objectives presented in Section 8.2, and a control-oriented model (COM) is used. The second controller consists in an optimization-based controller that does not consider a model of the system. With this approach, the behavioral tendency of the volumes with respect to the inflows is considered, i.e., taking into account that the inflows might induce the increment of tanks volumes. Finally, due to the fact that the large-scale case study (BDWN) has been controlled with model predictive control (MPC), reported in different works as in [18–21], then the performance of the designed controllers with the proposed population and mass dynamics approach is compared with the performance obtained with an MPC controller.

Moreover, physical constraints for tanks and control actions are considered, i.e., limitations over volumes and flows. These physical constraints are of the form

$$\begin{aligned} \mathbf{v}_{min} &\leq \mathbf{v}(k) \leq \mathbf{v}_{max}, \quad \text{for all } k, \\ \mathbf{x}_{min} &\leq \mathbf{x}(k) \leq \mathbf{x}_{max}, \quad \text{for all } k. \end{aligned}$$

8.3.1 Optimal control based on population dynamics using a control-oriented model

The design of a controller based on the proposed population and mass dynamics approach is presented by using a COM. Let us consider the COM shown in (16). The model may be expressed in terms of the elements at each population as follows:

$$\mathbf{v}^p(k+1) = \mathbf{A}^p \mathbf{v}^p(k) + \sum_{q \in \mathcal{P}} \mathbf{B}^q \mathbf{x}^q(k) + \mathbf{B}_I^p \mathbf{d}^p(k), \quad \text{for all } p \in \mathcal{P}, \quad (17a)$$

$$\mathbf{0} = \mathbf{E}_x^p \mathbf{x}^p(k) + \mathbf{E}_d^p \mathbf{d}^p(k), \quad \text{for all } p \in \mathcal{P}. \quad (17b)$$

² These costs are expressed in economic units (e.u.) instead of in the real value (euro) because of confidentiality reasons.

Then, an optimization problem that minimizes the objectives presented in Section 8.2, and that considers the model in (17) can be stated as follows:

$$\underset{\mathbf{x}^p, \boldsymbol{\xi}^p}{\text{maximize}} \quad -f(\mathbf{x}^p(k), \boldsymbol{\xi}^p(k)) = -\gamma_1(\alpha_1^p + \alpha_2^p(k))^\top \mathbf{x}^p(k) - \gamma_2 \boldsymbol{\xi}^p(k)^\top \boldsymbol{\xi}^p(k) - \gamma_3 \boldsymbol{\Delta} \mathbf{x}^p(k)^\top \boldsymbol{\Delta} \mathbf{x}^p(k), \quad (18a)$$

$$\text{subject to} \quad \mathbf{E}_x^p \mathbf{x}^p(k) + \mathbf{E}_d^p \mathbf{d}^p(k) = \mathbf{0}, \quad (18b)$$

$$\mathbf{v}_{min}^p \leq \mathbf{v}^p(k+1) \leq \mathbf{v}_{max}^p, \quad (18c)$$

$$\mathbf{x}_{min}^p \leq \mathbf{x}^p(k) \leq \mathbf{x}_{max}^p, \quad (18d)$$

$$\mathbf{v}^p(k+1) \geq \mathbf{v}_s^p - \boldsymbol{\xi}^p(k). \quad (18e)$$

Let $\mathbf{E}^p(k) = \mathbf{A}^p \mathbf{v}^p(k) + \sum_{q \in \mathcal{P}, q \neq p} \mathbf{B}^q \mathbf{x}^q(k-1) + \mathbf{B}_I^p \mathbf{d}^p(k)$ allow to use a COM. Finally, the whole optimization problem (18) can be written as follows:

$$\underset{\mathbf{x}^p, \boldsymbol{\xi}^p}{\text{maximize}} \quad -f(\mathbf{x}^p(k), \boldsymbol{\xi}^p(k)) = - \underbrace{\begin{bmatrix} \mathbf{x}^p(k) \\ \boldsymbol{\xi}^p(k) \end{bmatrix}^\top \begin{bmatrix} \gamma_3 \mathbb{I}_{N_x} & \mathbf{0} \\ \mathbf{0} & \gamma_2 \mathbb{I}_{N_v} \end{bmatrix} \begin{bmatrix} \mathbf{x}^p(k) \\ \boldsymbol{\xi}^p(k) \end{bmatrix}}_{\mathbf{W}} + \underbrace{\begin{bmatrix} 2\gamma_3 \begin{pmatrix} \mathbf{x}^p(k-1) \\ \mathbf{0} \end{pmatrix} - \gamma_1 \begin{pmatrix} \alpha_1^p + \alpha_2^p(k) \\ \mathbf{0} \end{pmatrix} \end{bmatrix}^\top \begin{bmatrix} \mathbf{x}^p(k) \\ \boldsymbol{\xi}^p(k) \end{bmatrix}}_{\mathbf{w}} \quad (19a)$$

$$- \gamma_3 \underbrace{\mathbf{x}(k-1)^\top \mathbf{x}(k-1)}_{\text{constant}},$$

$$\text{subject to} \quad \underbrace{\begin{bmatrix} \mathbf{E}_x^p(k) & \mathbf{0} \end{bmatrix}}_{\mathbf{H}} \begin{bmatrix} \mathbf{x}^p(k) \\ \boldsymbol{\xi}^p(k) \end{bmatrix} = \underbrace{-\mathbf{E}_d^p \mathbf{d}^p(k)}_{\mathbf{h}}, \quad (19b)$$

$$\underbrace{\begin{bmatrix} \mathbf{B}^p & \mathbf{0} \\ -\mathbf{B}^p & \mathbf{0} \end{bmatrix}}_{\mathbf{P}_1} \begin{bmatrix} \mathbf{x}^p(k) \\ \boldsymbol{\xi}^p(k) \end{bmatrix} \leq \underbrace{\begin{bmatrix} \mathbf{v}_{max}^p - \mathbf{E}^p(k) \\ -\mathbf{v}_{min}^p + \mathbf{E}^p(k) \end{bmatrix}}_{\mathbf{p}_1}, \quad (19c)$$

$$\underbrace{\begin{bmatrix} \mathbb{I}_{N_x} & \mathbf{0} \\ -\mathbb{I}_{N_x} & \mathbf{0} \end{bmatrix}}_{\mathbf{P}_2} \begin{bmatrix} \mathbf{x}^p(k) \\ \boldsymbol{\xi}^p(k) \end{bmatrix} \leq \underbrace{\begin{bmatrix} \mathbf{x}_{max}^p \\ -\mathbf{x}_{min}^p \end{bmatrix}}_{\mathbf{p}_2}, \quad (19d)$$

$$\underbrace{\begin{bmatrix} -\mathbf{B}^p & -\mathbb{I}_{N_v} \end{bmatrix}}_{\mathbf{P}_3} \begin{bmatrix} \mathbf{x}^p(k) \\ \boldsymbol{\xi}^p(k) \end{bmatrix} \leq \underbrace{\mathbf{E}^p(k) - \mathbf{v}_s^p}_{\mathbf{p}_3}. \quad (19e)$$

Consider the variable $\tilde{\mathbf{x}}^p(k) = [\mathbf{x}^p(k)^\top \quad \boldsymbol{\xi}^p(k)^\top]^\top$. Then, the cost function in the optimization problem (19) has the form $-f(\tilde{\mathbf{x}}^p) = -\tilde{\mathbf{x}}^p{}^\top \mathbf{W} \tilde{\mathbf{x}}^p + \mathbf{w}^\top \tilde{\mathbf{x}}^p - \text{constant}$, and the constraints have the form $\mathbf{H} \tilde{\mathbf{x}}^p = \mathbf{h}$, and $\mathbf{P} \tilde{\mathbf{x}}^p \leq \mathbf{p}$. Matrices \mathbf{P} and \mathbf{p} are composed of matrices $\mathbf{P}_1, \mathbf{P}_2, \mathbf{P}_3$, and $\mathbf{p}_1, \mathbf{p}_2, \mathbf{p}_3$, respectively. Then, a quadratic problem of the form (14) is obtained, and using Remark 4, it is solved with the proposed populations and mass dynamics approach.

8.3.2 Model-free optimal control based on population dynamics

This section presents the design of a controller without considering the model of the system, but just by considering the fact that the error within a tank (i.e., the difference between the safety value and the current volume) can be reduced as the control action is increased. In order to design a model-free controller based on the proposed methodology, it is defined a cost function corresponding to the desired behavior of the system. In this particular case, a volume error at each tank is considered.

The controller is designed through an optimization problem minimizing economical costs, the volume error with respect to the safety storage term, and variations in the control actions. These objectives are minimized subject to constraints of mass balance and physical constraints of actuators. To this end, new variables $\tilde{\mathbf{v}}_s \in \mathbb{R}^{N_x}$ of safety values, and $\tilde{\mathbf{v}} \in \mathbb{R}^{N_x}$ composed of tank volumes, are introduced. Notice that the dimension of the new vectors of volumes

Table 3
Discrimination of economical costs for different control strategies.

Day	Total Cost in Economical Units (e.u.)							
	Population Dynamics Approach				Model Predictive Control			
	Scenario 1 With COM		Scenario 2 Model-free		Scenario 3 Matching COM		Scenario 4 Mismatching COM	
	Water	Energy	Water	Energy	Water	Energy	Water	Energy
1	37217.03	22414.76	45484.48	18409.34	37915.28	22096.12	44580.44	20222.35
2	30516.06	22322.49	41384.76	18131.81	28352.38	22235.15	35075.95	20277.75
3	30518.46	22322.37	40022.43	18791.73	28400.39	22288.11	35189.99	20276.93
4	30518.49	22322.34	40389.76	18387.35	28330.14	22219.59	35015.71	20301.10
Sum	128770.06	89381.98	167281.43	73720.23	122998.21	88838.97	149862.09	81078.17
Overall costs	218152.04		241001.66		211837.17		230940.23	

corresponds to the dimension of the vector of control actions, i.e., $\tilde{\mathbf{v}}_s, \tilde{\mathbf{v}}, \mathbf{x} \in \mathbb{R}^{N_x}$. For the case study shown in Figure 12, consider the variables $\tilde{\mathbf{v}} = [\tilde{v}_1 \ \tilde{v}_2 \ \dots \ \tilde{v}_{61}]^\top$, $\tilde{\mathbf{v}}_s = [\tilde{v}_{s,1} \ \tilde{v}_{s,2} \ \dots \ \tilde{v}_{s,61}]^\top$, and $\mathbf{x} = [x_1 \ x_2 \ \dots \ x_{61}]^\top$. The scalar \tilde{v}_i denotes the volume corresponding to the tank whose inflow is given by x_i , and null in case that x_i is not an inflow for any tank. The safety volume $\tilde{v}_{s,i}$ corresponds to the safety volume of the tank whose inflow is given by x_i , and null otherwise. Briefly, $\tilde{v}_i = v_j$, and $\tilde{v}_{s,i} = v_{s,j}$ if x_i is the inflow of the j^{th} tank, and null if x_i is not an inflow for any tank (e.g., $\tilde{v}_4 = v_1$, and $\tilde{v}_2 = 0$). Notice that the constraints over the system states (i.e., tanks volumes) may not be considered since this approach does not use a COM. The following optimization problem only depends on measured state values (volumes) and decision variables (control actions):

$$\begin{aligned} & \underset{\mathbf{x}^p}{\text{maximize}} \quad -f(\mathbf{x}^p(k)) = -\gamma_1(\alpha_1^p + \alpha_2^p(k))^\top \mathbf{x}^p(k) - \gamma_2(\tilde{\mathbf{v}}_s^p - \tilde{\mathbf{v}}^p(k))^\top \text{diag}(\mathbf{x}^p(k))(\tilde{\mathbf{v}}_s^p - \tilde{\mathbf{v}}^p(k)) - \gamma_3 \Delta \mathbf{x}^p(k)^\top \Delta \mathbf{x}^p(k), \\ & \text{subject to} \quad \mathbf{E}_x^p \mathbf{x}^p(k) = -\mathbf{E}_d^p \mathbf{d}^p(k), \\ & \quad \quad \quad \begin{bmatrix} \mathbb{I}_{N_x} \\ -\mathbb{I}_{N_x} \end{bmatrix} \mathbf{x}^p(k) \leq \begin{bmatrix} \mathbf{x}_{max}^p \\ -\mathbf{x}_{min}^p \end{bmatrix}. \end{aligned}$$

Finally, the addition of slack variables may be used to make the problem to have the form (14).

9 Results and discussion

In order to analyze the proposed methodology, four different scenarios are proposed, two of them designed with the proposed population and mass dynamics approach and two of them by using a centralized MPC approach:

- *Scenario 1*: consists in a controller based on the proposed population and mass dynamics, and considering a COM.
- *Scenario 2*: consists in a model-free controller based on the proposed population and mass dynamics.
- *Scenario 3*: consists in an MPC controller with perfect COM (i.e., the COM equal to the SOM) and with a prediction horizon of one day $H_p = 24$.
- *Scenario 4*: consists in an MPC controller whose COM does not correspond to the SOM (i.e., with a subtle modification over the COM) and with a prediction horizon $H_p = 24$.

It is worth to highlight that the MPC controller with an imperfect COM is presented in order to make a fair comparison with respect to the model-free control approach with population dynamics.

Simulations are made by using the simulation-oriented model (SOM) shown in (16), and with real historical data for the disturbances. Scenarios consider the following parameters according to the given prioritization. The weights for the cost function are selected to be $\gamma_1 = 100$, $\gamma_2 = 10$, and $\gamma_3 = 1$. Initial conditions for simulations are chosen arbitrarily with respect to the safety volumes, i.e., $\mathbf{v}(0) = 0.5\mathbf{v}_s$.

According to the assigned prioritization of the management objectives, the most important one is to minimize is the economical aspect, hence $\gamma_1 = 100$. Table 3 shows the water costs whose minimization is a global objective since the

Table 4

Discrimination of cost function. i.e., economical costs, safety volume, and smooth operation ($f_1(\mathbf{x}(k)) + f_2(\boldsymbol{\xi}(k)) + f_3(\mathbf{x}(k))$).

Day	Population Dynamics Approach		Model Predictive Control	
	Scenario 1	Scenario 2	Scenario 3	Scenario 4
	With COM	Model-free	Matching COM	Mismatching COM
1	85753.68	90016.18	86136.48	105631.03
2	57412.11	64084.36	57776.91	94060.01
3	52937.18	58910.22	53723.53	80201.20
4	52889.09	58826.09	53529.68	66925.18
Overall costs	248992.02	271836.84	251166.61	346817.42

water sources can supply tanks of different cliques throughout the network. Table 3 also shows energy costs whose minimization is a local objective since these costs only depend on the local operation of each actuator within each clique. These economical costs are shown for the four different scenarios. It can be seen that the total economical cost of Scenario 1 is similar to the total economical cost of the Scenario 3. Moreover, economical costs for the Scenario 2 are similar to the costs with the Scenario 4. In both cases a better economical costs reduction is obtained with the MPC controllers. However, the MPC controllers dispose of full information in a centralized manner, and they also dispose of information of disturbances within the prediction horizon through a forecasting model (see [26] and references therein). In contrast, the distributed population and mass dynamics control approaches only possess of measured local information.

Now, the different controllers are compared by considering the whole cost function. Notice that, this comparison is more proper in the sense that the reduction of all objectives is considered. Table 4 shows the values for the whole cost function, i.e., considering the economical aspect, the safety volume, and the smooth operation. In these results, a better performance with the Scenario 2 can be seen, compared to the performance with the Scenario 4. Moreover, the proposed distributed approach requires less information than the MPC approach.

Figures 14a), 14b), and 14c) show the evolution of volumes of some tanks from the vector of all the volumes $\mathbf{v}(k)$. The behavior of the states is quite oscillatory (mostly for the MPC controller) due to the hard disturbances given by the demand profiles. As an example of these disturbances, Figure 15 shows the demand d_{21} .

Moreover, Figures 14a), 14b), and 14c) show that the distributed controllers based on populations and mass dynamics provoke less oscillations over the systems states. On the other hand, Figures 14d), 14e), and 14f) show the evolution of some control actions from the proportion of agents $\mathbf{x}(k)$ and the time-varying costs associated to them. For instance, Figure 14d) shows a quite similar behavior of the control signal. This oscillatory behavior is obtained because the control action corresponds to the inflow to a mass balance node that contains an outflow given by a demand, forcing the control action to have a similar pattern. The control action shown in Figure 14e) shows that, for the MPC controller, the flow x_{42} is the only inflow of the tank with volume v_{13} . The flow x_{42} is increased when the control action is cheaper, and it is reduced when the control action becomes more expensive. This desired behavior is obtained due to the fact that the MPC controller dispose of information about the behavior of the demand d_{19} within a time window of a day. In contrast, the controllers designed with the population and mass dynamics do not consider the behavior of d_{19} since they compute the control action x_{42} based only on measurements in the time instant k , and due to the fact that this control action is the only inflow able to modify the volume v_{13} , then a different performance with respect to the MPC controller is obtained. Finally, Figure 14f) shows the control action x_{48} , which is an inflow to tank with volume v_{17} . This is not the only inflow to this tank, i.e., control action x_{60} is also an inflow of the tank with volume v_{17} . In order to analyze the performance of the control action x_{48} , it is important to point out that the control action x_{60} is cheaper than x_{48} , and consequently the safety level at this tank is mostly achieved by using the cheaper inflow. Notice that, for all the controllers, the control action x_{48} is increased when its operation gets cheaper and it is reduced when its operational costs increase.

10 Concluding remarks

A methodology to solve different optimization problems with multiple constraints has been presented. The method is based on population dynamics, whose set of states varies over time (i.e., dynamics over the population masses are added). The variation of the set of possible states represents a mass interchange among populations. It has

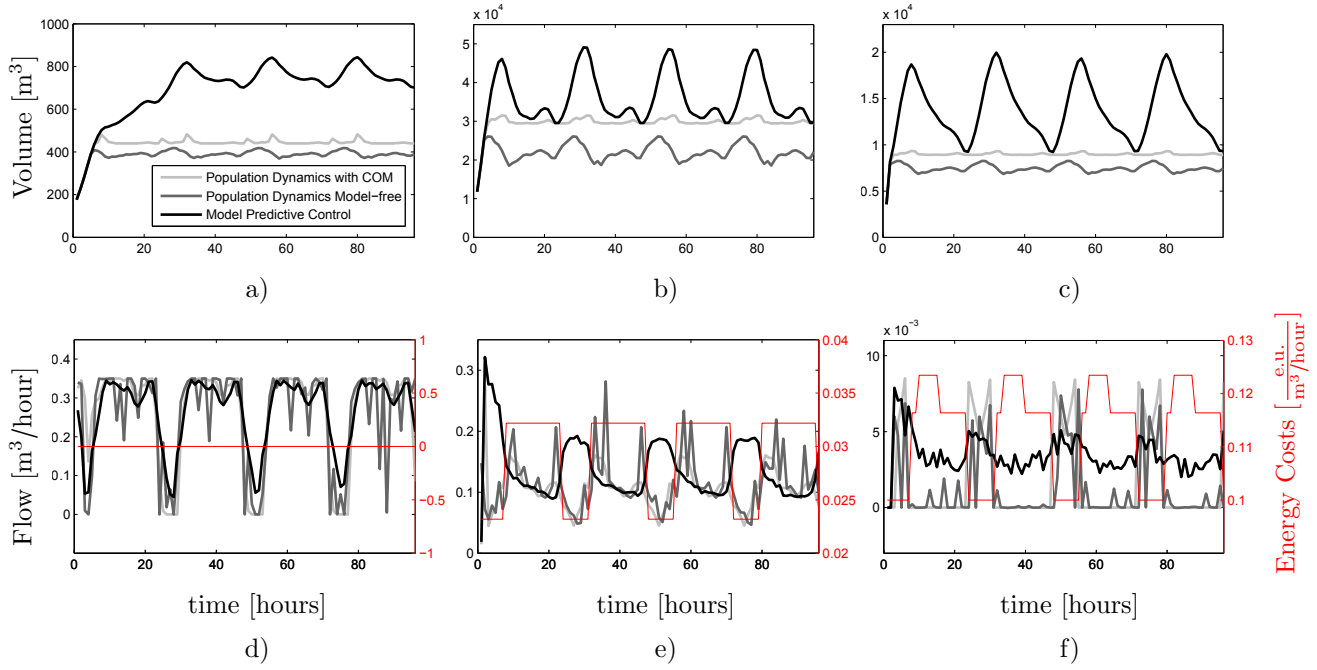


Fig. 14. Evolution of the volumes a) 2, b) 12, and c) 14. Evolution of the control actions d) 32, e) 42, and f) 48, with their corresponding costs.

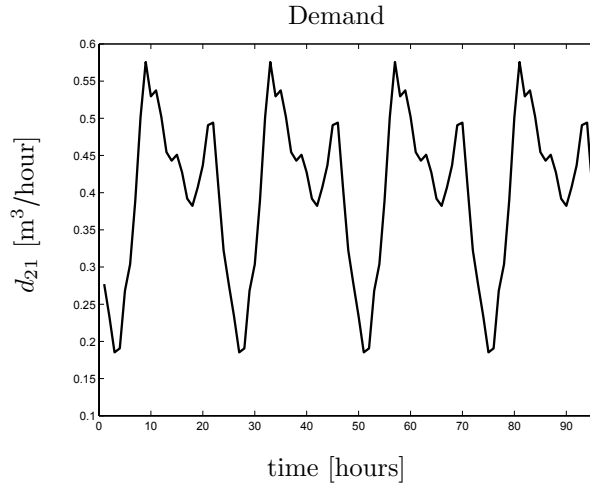


Fig. 15. Demand profile C100BLLnord.

been shown that the population dynamics and the mass dynamics are stable and that the feasible region of the global problem is attractive, under the presented assumptions associated to the objective function (i.e., the potential function of the game is concave).

The proposed distributed decision-making approach allows to design optimization-based systems where there are dynamical modifications over the graph that represents the society, without having to ensure that initial conditions satisfy the constraints. Notice that, in order to guarantee that the initial condition belongs to the feasible set, it would be required to have complete information about the system. In contrast, the proposed methodology allows to initialize the element values within the distributed system at any value in \mathbb{R}_+ . Additionally, it has been shown that changes in the topology of the network (e.g., the addition and/or removal of vertices and/or edges) imply only partial and local modifications in the decision-making system. Finally, the proposed approach has been applied in the design of distributed optimization-based controllers for a real case study, showing its effectiveness in comparison with already reported control strategies. As further work, it is of interest to analyze the proposed methodology in discrete

time in order to motivate its implementation, i.e., how the discrete version of the population and mass dynamics would be, and which conditions have to be satisfied in order to guarantee stability and convergence conditions.

Acknowledgements

We would like to thank Germán Obando for his inputs and the academic discussions about this work.

References

- [1] G. Arslan and J. Shamma. Distributed convergence to Nash equilibria with local utility measurements. In *Proceedings of the 43rd IEEE Conference on Decision and Control (CDC)*, pages 1538–1543, Atlantis, Paradise Island, Bahamas, 2004.
- [2] J. Barreiro-Gomez, N. Quijano, and C. Ocampo-Martinez. Constrained distributed optimization based on population dynamics. In *Proceedings of the 53rd IEEE Conference on Decision and Control (CDC)*, pages 4260–4265, Los Angeles, California, USA, 2014.
- [3] J. Barreiro-Gomez, N. Quijano, and C. Ocampo-Martinez. Distributed control of drinking water networks using population dynamics: Barcelona case study. In *Proceedings of the 53rd IEEE Conference on Decision and Control (CDC)*, pages 3216–3221, Los Angeles, California, USA, 2014.
- [4] D. Bertsekas. *Optimization for Machine Learning*, chapter Incremental gradient, subgradient and proximal methods for convex optimization: a survey, pages 85–119. MIT Press, 2012.
- [5] L. Gao and D. Cheng. Comment on coordination of groups of mobile autonomous agents using nearest neighbor rules. *IEEE Transactions on Automatic Control*, 50(11):1913–1916, 2005.
- [6] B. Gharesifard and J. Cortes. Distributed convergence to Nash equilibria in two-network zero-sum games. *Automatica*, 49:1683–1692, 2013.
- [7] J.M. Grosso, C. Ocampo-Martinez, and V. Puig. A service reliability model predictive control with dynamic safety stocks and actuators health monitoring for drinking water networks. In *Proceedings of the 51st IEEE Conference on Decision and Control (CDC)*, pages 4568–4573, Maui, Hawaii, USA, 2012.
- [8] J. Hofbauer and W. H. Sandholm. Stable games and their dynamics. *Journal of Economic Theory*, 144(4):1665–1693, 2009.
- [9] A. Jadbabaie, A.E. Ozdaglar, and M. Zargham. A distributed Newton method for network optimization. In *Proceedings of the 48th IEEE Conference on Decision and Control (CDC)*, pages 2736–2741, Shanghai, China, 2009.
- [10] B. Johansson, T. Keviczky, M. Johansson, and K.H. Johansson. Subgradient methods and consensus algorithms for solving convex optimization problems. In *Proceedings of the 47th IEEE Conference on Decision and Control (CDC)*, pages 4185–4190, Cancun, Mexico, 2008.
- [11] N. Li and J. Marden. Designing games for distributed optimization with a time varying communication graph. In *Proceedings of the 51st IEEE Conference on Decision and Control (CDC)*, pages 7764–7769, Maui, Hawaii, USA, 2012.
- [12] N. Li and J. Marden. Designing games for distributed optimization. *IEEE Journal of Selected Topics in Signal Processing*, 7(2):230–242, 2013.
- [13] N. Li and J. Marden. Decoupling coupled constraints through utility design. *Transactions on Automatic Control*, 59(8):2289–2294, 2014.
- [14] J. Marden. State based potential games. *Automatica*, 48:3075–3088, 2012.
- [15] J. Marden and J. Shamma. *Game theory and distributed control*, volume 4, chapter Handbook of Game Theory with Economic Applications, pages 861–899. Elsevier, 2015.
- [16] G. Notarstefano and F. Bullo. Distributed abstract optimization via constraint consensus: Theory and applications. *IEEE Transactions on Automatic Control*, 56(10):2247–2261, 2011.
- [17] M.A. Nowak. *Evolutionary Dynamics*. Harvard University Press, 2006.
- [18] C. Ocampo-Martinez, D. Barcelli, V. Puig, and A. Bemporad. Hierarchical and decentralised model predictive control of drinking water networks: application to Barcelona case study. *IET Control Theory and Applications*, 6(1):62–71, 2012.
- [19] C. Ocampo-Martinez, S. Bovo, and V. Puig. Partitioning approach oriented to the decentralised predictive control of large-scale systems. *Journal of Process Control*, 21:775–786, 2011.
- [20] C. Ocampo-Martinez, V. Puig, G. Cembrano, R. Creus, and M. Minoves. Improving water management efficiency by using optimization-based control strategies: the Barcelona case study. *Water Science & Technology: Water Supply*, 9(5):565–575, 2009.
- [21] C. Ocampo-Martinez, V. Puig, G. Cembrano, and J. Quevedo. Application of predictive control strategies to the management of complex networks in the urban water cycle. *IEEE Control Systems Magazine*, 33(1):15–41, 2013.
- [22] A. Pantoja and N. Quijano. A population dynamics approach for the dispatch of distributed generators. *IEEE Transactions on Industrial Electronics*, 58(10):4559–4567, 2011.
- [23] W.H. Sandholm. *Population games and evolutionary dynamics*. Cambridge, Mass. MIT Press, 2010.
- [24] A. Simonetto, T. Keviczky, and R. Babuska. Distributed non-linear estimation for robot localization using weighted consensus. In *Proceedings of the IEEE International Conference on Robotics and Automation*, pages 3026–3031, 2010.

- [25] A. Simonetto, T. Keviczky, and R. Babuska. On distributed maximization of algebraic connectivity in robotic networks. In *Proceedings of the American Control Conference (ACC)*, pages 2180–2185, San Francisco, California, USA, 2011.
- [26] Y. Wang, C. Ocampo-Martinez, and V. Puig. Robust model predictive control based on gaussian processes: Application to drinking water networks. In *Proceedings of the European Control Conference (ECC)*, Linz, Austria, 2015.
- [27] E. Wei, A.E. Ozdaglar, and A. Jadbabaie. A distributed Newton method for network utility maximization-I: Algorithm. *IEEE Transactions on Automatic Control*, 58(9):2162–2175, 2013.
- [28] J. Zhang, D. Qi, and G. Zhao. A game theoretical formulation for distributed optimization problems. In *IEEE 10th International Conference on Control and Automation (ICCA)*, pages 1939–1944, Hangzhou, China, 2013.
- [29] X. Zhang and X. Liu. Consensus of second-order multi-agent systems with disturbances generated by non-linear exosystems under switching topologies. *Journal of the Franklin Institute*, 35(1):473–486, 2014.
- [30] M. Zhu and S. Martinez. On distributed convex optimization under inequality and equality constraints. *IEEE Transactions on Automatic Control*, 57(1):151–164, 2012.



Julian Barreiro-Gomez received his B.S. degree in Electronics Engineering from Universidad Santo Tomas (USTA), Bogotá, Colombia, in 2011. He received the MSc. degree in Electrical Engineering from Universidad de Los Andes (UAndes), Bogotá, Colombia, in 2013. Since 2012, he is with the research group in control and automation systems (GIAP, UAndes), where he is pursuing the Ph.D. degree in Engineering in the area of control systems. Since 2014, he is associate researcher at Technical University of Catalonia (Barcelona, Spain), Automatic Control Department (ESAII), and Institut de Robòtica i Informàtica Industrial (CSIC-UPC), where he is pursuing the Ph.D. degree in Automatic, Robotics and Computer Vision. His main research interests are constrained model predictive control, distributed optimization and control, game theory, and population dynamics.



Nicanor Quijano received his B.S. degree in Electronics Engineering from Pontificia Universidad Javeriana (PUJ), Bogotá, Colombia, in 1999. He received the M.S. and PhD degrees in Electrical and Computer Engineering from The Ohio State University, in 2002 and 2006, respectively. In 2007 he joined the Electrical and Electronics Engineering Department, Universidad de los Andes (UAndes), Bogotá, Colombia as Assistant Professor. In 2008 he obtained the Distinguished Lecturer Award from the School of Engineering, UAndes. He is currently Full Professor and the director of the research group in control and automation systems (GIAP, UAndes). On the other hand, he has been a member of the Board of Governors of the IEEE Control Systems Society (CSS) for the 2014 period, and he was the Chair of the IEEE CSS, Colombia for the 2011-2013 period.

Currently his research interests include: hierarchical and distributed optimization methods using bio-inspired and game-theoretical techniques for dynamic resource allocation problems, especially those in energy, water, and transportation. For more information and a complete list of publications see: <https://profesores.uniandes.edu.co/nquijano/>



Carlos Ocampo-Martinez received his electronics engineering degree and his MSc. degree in industrial automation from the National University of Colombia, Campus Manizales, in 2001 and 2003, respectively. In 2007, he received his Ph.D. degree in Control Engineering from the Technical University of Catalonia (Barcelona, Spain). In 2007-2008, he held a postdoctoral position at the ARC Centre of Complex Dynamic Systems and Control (University of Newcastle, Australia) and, afterwards at the Spanish National Research Council (CSIC), Institut de Robòtica i Informàtica Industrial, CSIC-UPC (Barcelona) as a *Juan de la Cierva* research fellow between 2008 and 2011. Since 2011, he is with the Technical University of Catalonia, Automatic Control Department (ESAII) as Associate Professor in automatic control and model predictive control. Since 2014,

he is also Deputy Director of the Institut de Robòtica i Informàtica Industrial (CSIC-UPC), a Joint Research Center of UPC and CSIC. His main research interests include constrained model predictive control, large-scale systems management (partitioning and non-centralized control), and industrial applications (mainly related to the key scopes of water and energy).